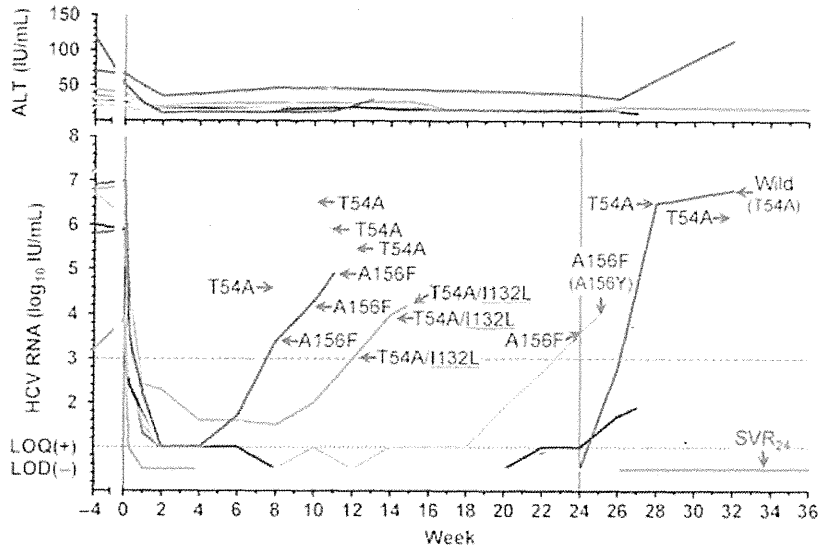

Fig. 4 Viral kinetics and predominant variants during and after telaprevir monotherapy beyond 8 weeks. Besides predominant clones, minority clones which account for 10% and more in a specimen are also summarized by brace notation. Putative secondary resistant-associated mutation is indicated by underline.

responsive to sequential therapy with PEG-IFN and RBV, the substitutions in the NS3 protease domain by the telaprevir treatment are not correlated with resistance to PEG-IFN and/or RBV directly as described previously [23,24]. Sequential therapy with PEG-IFN and RBV after relapse or viral breakthrough on telaprevir monotherapy might be a therapeutic option in some cases, including the case of low haemoglobin. By taking the error-prone nature of HCV replication into account, successful eradication with IFN-free DAA(s) regimens probably depends on how efficiently DAA can suppress various DAA-resistant variants that pre-exist and are selected under DAA pressure. The telaprevir-based combination therapy with other DAA(s) such as NS5A or NS5B polymerase inhibitors may be useful for successful treatment. Using a human chimeric liver mouse model for HCV infection, Ohara *et al.* [26] reported that the combination of telaprevir with a high-dose nucleoside analogue could successfully eradicate HCV infection. Recently, it was reported that the dual therapy with daclatasvir, an NS5A replication complex inhibitor, and asunaprevir, NS3-4A protease inhibitor, had high SVR rates in difficult-to-treat patients with subtype 1b and null responders [27,28]. These successful results are also helpful for us to consider telaprevir-based IFN-free regimens in combination with other DAAs against HCV.

In conclusion, telaprevir monotherapy was well tolerated and provided potent but temporary antiviral activity in Japanese patients with subtype 1b HCV, with an SVR rate of 7%. Most AEs were mild to moderate and much milder than those recorded in patients on combinations with PEG-IFN and RBV. As the essential characteristics of DAAs including telaprevir are substantially masked in the co-administration with other antivirals, the knowledge obtained from the long-term telaprevir monotherapy is most likely to contribute to the future HCV treatment with DAA-based regimens.

ACKNOWLEDGEMENT AND DISCLOSURES

Toyota J., Ozeki I., Karino Y., Asahina Y., Izumi N., Takahashi S., Kawakami Y., Chayama K., Suzuki Y., Suzuki F. and Kumada H. are none to declare. Kamiya N., Aoki K. and Yamada I. are employees of Mitsubishi Tanabe Pharma Corporation. Yuko Sakurai, Hidetomo Terai and Mitsuru Yoneyama assisted in the preparation of the article. All are employees of Mitsubishi Tanabe Pharma Corporation.

REFERENCES

1 World Health Organization. Fact sheet No.164 June 2011. Hepatitis C. Available at: http://www.who.int/mediacentre/factsheets/fs164/en/index.html (accessed 27 June 2011).
2 Jacobson IM, McHutchison JG, Dusheiko G *et al.* Telaprevir for previously untreated chronic hepatitis C virus infection. *N Engl J Med* 2011; 364: 2405–2416.
3 Zeuzem S, Andreone P, Pol S *et al.* Telaprevir for retreatment of HCV infection. *N Engl J Med* 2011; 364: 2417–2428.
4 Sherman KE, Flamm SL, Afdhal NH *et al.* Response-guided telaprevir combination treatment for hepatitis C virus infection. *N Engl J Med* 2011; 365: 1014–1024.
5 Kumada H, Toyota J, Okanoue T, Chayama K, Tsubouchi H, Hayashi N. Telaprevir with peginterferon and ribavirin for treatment-naive patients chronically infected with

HCV of genotype 1 in Japan. *J Hepatol* 2012; 56: 78–84.

6 Hayashi N, Okanoue T, Tsubouchi H, Toyota J, Chayama K, Kumada H. Efficacy and safety of Telaprevir, a new protease inhibitor, for difficult-to-treat patients with genotype 1 chronic hepatitis C. *J Viral Hepat* 2012; 19: 134–142.

7 Chung H, Ueda T, Kudo M. Changing trends in hepatitis C infection over the past 50 years in Japan. *Intervirology* 2010; 53: 39–43.

8 Okamoto H, Mishiro S. Genetic heterogeneity of hepatitis C virus. *Intervirology* 1994; 37: 68–76.

9 Kieffer TL, Sarrazin C, Miller JS *et al.* Telaprevir and pegylated interferon-alpha-2a inhibit wild-type and resistant genotype 1 hepatitis C virus replication in patients. *Hepatology* 2007; 46: 631–639.

10 Kuntzen T, Timm J, Berical A *et al.* Naturally occurring dominant resistance mutations to hepatitis C virus protease and polymerase inhibitors in treatment-naive patients. *Hepatology* 2008; 48: 1769–1778.

11 Yamada I, Suzuki F, Kamiya N *et al.* Safety, pharmacokinetics and resistant variants of telaprevir alone for 12 weeks in hepatitis C virus genotype 1b infection. *J Viral Hepat* 2012; 19: e112–e119.

12 Manns MP, Wedemeyer H, Cornberg M. Treating viral hepatitis C: efficacy, side effects, and complications. *Gut* 2006; 55: 1350–1359.

13 Oze T, Hiramatsu N, Yakushijin T *et al.* Indications and limitations for aged patients with chronic hepatitis C in pegylated interferon alfa-2b plus ribavirin combination therapy. *J Hepatol* 2011; 54: 604–611.

14 Huang CF, Yang JF, Dai CY *et al.* Efficacy and safety of pegylated interferon combined with ribavirin for the treatment of older patients with chronic hepatitis C. *J Infect Dis* 2010; 201: 751–759.

15 Suzuki F, Suzuki Y, Akuta N *et al.* Sustained virological response in a patient with chronic hepatitis C treated by monotherapy with the NS3-4A protease inhibitor telaprevir. *J Clin Virol* 2010; 47: 76–78.

16 McHutchison JG, Everson GT, Gordon SC *et al.* Telaprevir with peginterferon and ribavirin for chronic HCV genotype 1 infection. *N Engl J Med* 2009; 360: 1827–1838.

17 Hezode C, Forestier N, Dusheiko G *et al.* Telaprevir and peginterferon with or without ribavirin for chronic HCV infection. *N Engl J Med* 2009; 360: 1839–1850.

18 McHutchison JG, Manns MP, Muir AJ *et al.* Telaprevir for previously treated chronic HCV infection. *N Engl J Med* 2010; 362: 1292–1303.

19 Sarrazin C, Zeuzem S. Resistance to direct antiviral agents in patients with hepatitis C virus infection. *Gastroenterology* 2010; 138: 447–462.

20 Romano KP, Ali A, Royer WE, Schiffer CA. Drug resistance against HCV NS3/4A inhibitors is defined by the balance of substrate recognition versus inhibitor binding. *Proc Natl Acad Sci USA* 2010; 107: 20986–20991.

21 Lin C, Gates CA, Rao BG *et al.* In vitro studies of cross-resistance mutations against two hepatitis C virus serine protease inhibitors, VX-950 and BILN 2061. *J Biol Chem* 2005; 280: 36784–36791.

22 Zhou Y, Bartels DJ, Hanzelka BL *et al.* Phenotypic characterization of resistant Val^{36} variants of hepatitis C virus NS3-4A serine protease. *Antimicrob Agents Chemother* 2008; 52: 110–120.

23 Shimakami T, Welsch C, Yamane D *et al.* Protease inhibitor-resistant hepatitis C virus mutants with reduced fitness from impaired production of infectious virus. *Gastroenterology* 2011; 140: 667–675.

24 Sarrazin C, Kieffer TL, Bartels D *et al.* Dynamic hepatitis C virus genotypic and phenotypic changes in patients treated with the protease inhibitor telaprevir. *Gastroenterology* 2007; 132: 1767–1777.

25 Ozeki I, Akaike J, Karino Y *et al.* Antiviral effects of peginterferon alpha-2b and ribavirin following 24-week monotherapy of telaprevir in Japanese hepatitis C patients. *J Gastroenterol* 2011; 46: 929–937.

26 Ohara E, Hiraga N, Imamura M *et al.* Elimination of hepatitis C virus by short term NS3-4A and NS5B inhibitor combination therapy in human hepatocyte chimeric mice. *J Hepatol* 2011; 54: 872–878.

27 Chayama K, Takahashi S, Toyota J *et al.* Dual therapy with the nonstructural protein 5A inhibitor, daclatasvir, and the nonstructural protein 3 protease inhibitor, asunaprevir, in hepatitis C virus genotype 1b-infected null responders. *Hepatology* 2012; 55: 742–748.

28 Anna SL, Daid FG, Eric L *et al.* Preliminary study of two antiviral agents for hepatitis C genotype 1. *N Engl J Med* 2012; 366: 216–224.

OPEN ACCESS Freely available online

PLOS | ONE

Inhibition of Both Protease and Helicase Activities of Hepatitis C Virus NS3 by an Ethyl Acetate Extract of Marine Sponge *Amphimedon* sp.

Yuusuke Fujimoto[1], Kazi Abdus Salam[2☯], Atsushi Furuta[3,4☯], Yasuyoshi Matsuda[3,4], Osamu Fujita[3,4], Hidenori Tani[5], Masanori Ikeda[6], Nobuyuki Kato[6], Naoya Sakamoto[7], Shinya Maekawa[8], Nobuyuki Enomoto[8], Nicole J. de Voogd[9], Masamichi Nakakoshi[10], Masayoshi Tsubuki[10], Yuji Sekiguchi[3], Satoshi Tsuneda[4], Nobuyoshi Akimitsu[2], Naohiro Noda[3,4], Atsuya Yamashita[1]*, Junichi Tanaka[11]*, Kohji Moriishi[1]*

1 Department of Microbiology, Division of Medicine, Graduate School of Medicine and Engineering, University of Yamanashi, Yamanashi, Japan, **2** Radioisotope Center, The University of Tokyo, Tokyo, Japan, **3** Biomedical Research Institute, National Institute of Advanced Industrial Science and Technology, Ibaraki, Japan, **4** Department of Life Science and Medical Bioscience, Waseda University, Tokyo, Japan, **5** Research Institute for Environmental Management Technology, National Institute of Advanced Industrial Science and Technology, Ibaraki, Japan, **6** Department of Tumor Virology, Okayama University Graduate School of Medicine, Dentistry, and Pharmaceutical Sciences, Okayama, Japan, **7** Department of Gastroenterology and Hepatology, Hokkaido University Graduate School of Medicine, Sapporo, Japan, **8** First Department of Internal Medicine, Faculty of Medicine, University of Yamanashi, Yamanashi, Japan, **9** Netherlands Centre for Biodiversity Naturalis, Leiden, The Netherlands, **10** Institute of Medical Chemistry, Hoshi University, Tokyo, Japan, **11** Department of Chemistry, Biology and Marine Science, University of the Ryukyus, Okinawa, Japan

Abstract

Combination therapy with ribavirin, interferon, and viral protease inhibitors could be expected to elicit a high level of sustained virologic response in patients infected with hepatitis C virus (HCV). However, several severe side effects of this combination therapy have been encountered in clinical trials. In order to develop more effective and safer anti-HCV compounds, we employed the replicon systems derived from several strains of HCV to screen 84 extracts from 54 organisms that were gathered from the sea surrounding Okinawa Prefecture, Japan. The ethyl acetate-soluble extract that was prepared from marine sponge *Amphimedon* sp. showed the highest inhibitory effect on viral replication, with EC_{50} values of 1.5 and 24.9 μg/ml in sub-genomic replicon cell lines derived from genotypes 1b and 2a, respectively. But the extract had no effect on interferon-inducing signaling or cytotoxicity. Treatment with the extract inhibited virus production by 30% relative to the control in the JFH1-Huh7 cell culture system. The *in vitro* enzymological assays revealed that treatment with the extract suppressed both helicase and protease activities of NS3 with IC_{50} values of 18.9 and 10.9 μg/ml, respectively. Treatment with the extract of *Amphimedon* sp. inhibited RNA-binding ability but not ATPase activity. These results suggest that the novel compound(s) included in *Amphimedon* sp. can target the protease and helicase activities of HCV NS3.

Citation: Fujimoto Y, Salam KA, Furuta A, Matsuda Y, Fujita O, et al. (2012) Inhibition of Both Protease and Helicase Activities of Hepatitis C Virus NS3 by an Ethyl Acetate Extract of Marine Sponge *Amphimedon* sp.. PLoS ONE 7(11): e48685. doi:10.1371/journal.pone.0048685

Editor: Tetsuo Takehara, Osaka University Graduate School of Medicine, Japan

Received June 16, 2012; **Accepted** October 1, 2012; **Published** November 7, 2012

Funding: This work was supported in part by grants-in-aid from the Ministry of Health, Labor, and Welfare (http://www.mhlw.go.jp/) and from the Ministry of Education, Culture, Sports, Science, and Technology of Japan (http://www.mext.go.jp/). The funders had no role in study design, data collection and analysis, decision to publish, or preparation of the manuscript.

Competing Interests: The authors have declared that no competing interests exist.

* E-mail: atsuyay@yamanashi.ac.jp (AY); jtanaka@sci.u-ryukyu.ac.jp (JT); kmoriishi@yamanashi.ac.jp (KM)

☯ These authors contributed equally to this work.

Introduction

Hepatitis C virus (HCV) is an enveloped RNA virus of the genus *Hepacivirus* of the *Flaviviridae* family. More than 170 million patients persistently infected with HCV have been reported worldwide, leading to liver diseases including steatosis, cirrhosis, and hepatocellular carcinoma [1,2]. The genome of HCV is characterized as a single positive-strand RNA with a nucleotide length of 9.6 kb, flanked by 5′ and 3′-untranslated regions (UTRs). The genomic RNA encodes a large polyprotein consisting of approximately 3,000 amino acids [3], which is translated under the control of an internal ribosome entry site (IRES) located within the 5′-UTR of the genomic RNA [4]. The translated polyprotein is cleaved by host and viral proteases, resulting in 10 mature viral proteins [3]. The structural proteins, consisting of core, E1, and E2, are located in the N-terminal quarter of the polyprotein, followed by viroporin p7, which has not yet been classified into a structural or nonstructural protein. Further cleavage of the remaining portion by viral proteases produces six nonstructural proteins–NS2, NS3, NS4A, NS4B, NS5A, and NS5B–which form a viral replication complex with various host factors. The viral protease NS2 cleaves its own C-terminal between NS2 and NS3. After that, NS3 cleaves the C-terminal ends of NS3 and NS4A and then forms a complex with NS4A. The NS3/4A complex becomes a fully active form to cleave the C-terminal parts of the polyprotein, including nonstructural proteins. NS3 also possesses

RNA helicase activity to unwind the double-stranded RNA during the synthesis of genomic RNA [5,6].

Although the previous standard therapy, combining pegylated interferon with ribavirin, was effective in only about half of patients infected with genotype 1, the most common genotype worldwide [7–9], recent biotechnological advances have led to the development of a novel therapy using anti-HCV agents that directly target HCV proteins or host factors required for HCV replication and have improved the sustained virologic response (SVR) [10–12]. Telaprevir and boceprevir, which are categorized as advanced NS3/4A protease inhibitors, were recently approved for the treatment of chronic hepatitis C patients infected with genotype 1 [13,14]. The triple combination therapy with pegylated interferon, ribavirin, and telaprevir improved SVR by 77% in patients infected with genotype 1 [15]. However, this therapy exhibits side effects including rash, severe cutaneous eruption, influenza-like symptoms, cytopenias, depression, and anemia [7,16,17]. Furthermore, the possibility of the emergence of drug-resistant viruses is a serious problem with therapies that use antiviral compounds [18,19].

Recent technical advances in the determination of molecular structures and the synthesis of chemical compounds have led to the development of various drugs based on natural products, especially drugs identified from terrestrial plants and microbes [20–22]. Marine organisms, including plants and animals, were recently established as representative of a natural resource library for drug development. Potent biological activity is often found in products isolated from marine organisms because of their novel molecular structures [23,24]. Trabectedin (Yondelis), cytarabine (Ara-C), and eribulin (Halaven), which are known as antitumor drugs, were developed from compounds found in marine organisms [25].

In this study, we screened 84 extracts prepared from 54 marine organisms by using replicon cell lines derived from HCV genotype 1b and attempted to identify the extract that inhibits HCV RNA replication. A marine organism may produce anti-HCV agent(s) that could inhibit the protease and helicase activities of NS3.

Results

Effect of the Extract from Marine Sponge and Tunicate on HCV Replication

We prepared methanol (MeOH)- and ethyl acetate (EtOAc)-soluble extracts from 54 marine organisms in order to test which of these extracts could best suppress HCV replication. Each extract was added at 25 μg/ml to the culture supernatant of HCV replicon cell lines derived from O and Con1 strains of genotype 1b, which produce the luciferase/neomycin hybrid protein depending on RNA replication. Luciferase activity and cell viability were measured 72 h after treatment with the extracts (Table 1). The extracts exhibiting more than 85% cell viability and lower than 15% luciferase activity were selected as arbitrary candidates for the extract including anti-HCV compounds. The EtOAc-extract prepared from sample C-29 (C-29EA) was selected as a candidate in both cell lines. Thus, the anti-HCV activity of extract C-29EA was tested.

The EtOAc-soluble extract C-29EA was prepared from the marine sponge *Amphimedon* sp. (Fig. 1A), which inhabits the sea surrounding Okinawa Prefecture, Japan. HCV replication was inhibited in a dose-dependent manner but did not exhibit cytotoxicity when replicon cells were treated with C-29EA (Fig. 1 B). The extract C-29EA exhibited EC_{50} values of 1.5 μg/ml (Table 2). Furthermore, treatment with C-29EA suppressed the HCV replication derived from the genotype 2a strain JFH1 with an EC_{50} of 24.9 μg/ml, irrespective of cell viability (Fig. 2A and Table 2). Extract C-29EA also inhibited the production of infectious viral particles, viral RNA, and core protein from JFH1-infected cells in the supernatant (Fig. 2B and C). These results suggest that the marine sponge *Amphimedon* sp. possesses anti-HCV agents.

Effect of Extract C-29EA on IRES-dependent Translation

Extract C-29EA had the most potent inhibitory activity against HCV replication. The viral replication (Fig. 1 B and 2 A) and viral proteins (Fig. 3 A and B) in replicon cell lines derived from genotype 1b strain Con1 and 2a strain JFH1 were decreased 72 h after treatment in a dose-dependent manner. HCV protein has been translated based on the positive-sense viral RNA in an IRES-dependent manner. The replicon RNA of HCV is composed of the 5′-UTR of HCV, indicator genes (a luciferase-fused drug-resistant gene), encephalomyocarditis virus (EMCV) IRES, the viral genes encoding complete or nonstructural proteins, and the 3′-UTR of HCV, in that order [26]. The replicon RNA replicated autonomously in several HCV replication-permissive cell lines derived from several hepatoma cell lines. Nonstructural proteins in replicon cells were polycistronically translated through EMCV IRES. The cap-dependent translated mRNA, including *Renilla* luciferase, EMCV IRES, and the firefly luciferase/neomycin-resistant gene, in that order, was constructed to examine the effect of the extract on EMCV-IRES-dependent translation (Fig. 3C). When the mRNA expression was transcribed by an EF promoter of the transfected plasmid in the presence of C-29EA, the ratio of firefly luciferase activity to *Renilla* luciferase activity was not changed (Fig. 3C). This suggested that treatment with C-29EA exhibited no effect on EMCV-IRES-dependent translation. Furthermore, treatment with C-29EA did not significantly affect the activity of HCV IRES that was used instead of EMCV IRES in the system described above (Fig. 3D). Thus, these results suggest that treatment with C-29EA exhibits no effect on EMCV- or HCV-IRES-dependent translation.

Effect of C-29EA on the Interferon Signaling Pathway

It has been well known that HCV replication in cultured cells is potently inhibited by interferon [27,28]. We examined whether or not treatment with C-29EA elicits an interferon-inducible gene from replicon cells. The replicon cells were treated with various concentrations of interferon-alpha 2b or 15 μg of C-29EA per milliliter. The treated cells were harvested at 72 h post-treatment. The interferon-inducible gene 2′, 5′-OAS, was induced with IFN-alpha 2b but not with a 10-times EC_{50} concentration of C-29EA (Fig. 4). These results suggest that the inhibitory effect of C-29EA on the replication of the HCV replicon is independent of the IFN signaling pathway.

Effect of C-29EA on the NS3 Helicase Activity

We previously established an assay system for unwinding HCV activity based on photoinduced electron transfer (PET) [29,30]. The fluorescent dye (BODIPY FL) is attached to the cytosine at the 5′-end of the fluorescent strand and quenched by the guanine base at the 3′-end of the complementary strand via PET. When helicase unwinds the double-strand RNA substrate, the fluorescence of the dye emits a bright light upon the release of the dye from the guanine base. The capture strand, which is complementary to the complementary strand, prevents the reannealing of the unwound duplex. Treatment with C-29EA inhibited the helicase activity in a dose-dependent manner, with an IC_{50} value of 18.9 μg/ml (Fig. 5A). We confirmed the effect of C-29EA on NS3 helicase unwinding activity by the RNA helicase assay using ^{32}P-labeled double-stranded RNA (dsRNA) as a substrate. Treatment

Table 1. Effect of marine organism extracts on HCV replication and cell viability.

No.	Sample	Luciferase activity (% of control)		Cell viability (% of control)		Phylum	Specimen	Extract	Site
		O	Con1	O	Con1				
1	A-1	10	111	105	104	Sponge	*Unidentified*	MeOH	A
2	A-2	82	209	91	132	Soft coral	*Briareum*	MeOH	A
3	A-3	87	177	54	110	Tunicate	*unidentified*	MeOH	A
4	A-4	82	186	84	100	Sponge	*Liosina*	MeOH	A
5	B-5	110	165	86	110	Sponge	*unidentified*	MeOH	B
6	B-6	70	149	103	119	Sponge	*Xestospongia*	MeOH	B
7	B-7	89	191	111	144	Sponge	*Epipolasis*	MeOH	B
8	B-8	89	182	115	132	Sponge	*unidentified*	MeOH	B
9	B-9	57	72	92	124	Sponge	*Strongylophora*	MeOH	B
10	B-10	106	182	73	96	Sponge	*Stylotella aurantium*	MeOH	B
11	C-12	96	162	114	98	Sponge	*Epipolasis*	MeOH	B
12	C-13	123	141	91	103	Sponge	*unidentified*	MeOH	B
13	C-14	89	175	77	100	Sponge	*Hippospongia*	MeOH	B
14	C-16	80	177	108	88	Sponge	*unidentified*	MeOH	B
15	C-18	119	170	93	94	Sponge	*unidentified*	MeOH	B
16	C-19	0	0	0	4	Sponge	*unidentified*	MeOH	B
17	C-20	101	158	61	106	Sponge	*Xestospongia testudinaria*	MeOH	B
18	C-21	85	161	83	102	Sponge	*unidentified*	MeOH	B
19	C-22	109	88	38	89	Sponge	*unidentified*	MeOH	B
20	C-23	94	156	32	90	Sponge	*unidentified*	MeOH	B
21	C-24	118	86	42	94	Sponge	*Theonella*	MeOH	B
22	C-25	82	111	91	106	Sponge	*unidentified*	MeOH	B
23	C-27	0	0	15	2	Sponge	*unidentified*	MeOH	B
24	C-28	90	166	30	90	Sponge	*Petrosia*	MeOH	B
25	C-29	65	151	29	101	Sponge	*Amphimedon*	MeOH	B
26	D-31	81	127	55	91	Tunicate	*unidentified*	MeOH	C
27	D-32	80	141	47	93	Sponge	*unidentified*	MeOH	C
28	D-33	88	153	72	90	Gorgonian	*Junceella fragilis*	MeOH	C
29	E-35	114	156	40	118	Sponge	*Phyllospongia sp.*	MeOH	C
30	E-36	80	125	69	116	Tunicate	*Didemnum molle*	MeOH	C
31	E-37	88	129	54	108	Sponge	*Xestospongia sp.*	MeOH	C
32	E-38	70	153	35	112	Sponge	*unidentified*	MeOH	C
33	F-40	119	170	38	104	Sponge	*unidentified*	MeOH	C
34	F-41	88	166	48	101	Soft coral	*unidentified*	MeOH	C
35	G-42	113	157	31	126	Sponge	*unidentified*	MeOH	D
36	H-43	83	0	39	5	Sponge	*unidentified*	MeOH	D
37	J-44	62	183	27	105	Sponge	*Cinachyra*	MeOH	D
38	J-45	96	140	47	103	Sponge	*Liosina*	MeOH	D
39	J-46	83	149	77	102	Sponge	*unidentified*	MeOH	D
40	J-47	94	37	40	111	Sponge	*unidentified*	MeOH	D
41	J-48	24	16	53	70	Sponge	*Stylotella*	MeOH	D
42	J-49	78	123	55	105	Sponge	*unidentified*	MeOH	D
43	J-50	93	138	51	108	Sponge	*unidentified*	MeOH	D
44	J-51	103	73	41	115	Sponge	*unidentified*	MeOH	D
45	J-52	162	237	113	131	Sponge	*unidentified*	MeOH	D
46	J-53	51	90	93	122	Tunicate	*Didemnum*	MeOH	D
47	J-54	42	90	113	124	Sponge	*unidentified*	MeOH	D

Table 1. Cont.

No.	Sample	Luciferase activity (% of control)		Cell viability (% of control)		Phylum	Specimen	Extract	Site
		O	Con1	O	Con1				
48	J-55	88	133	131	110	Jellyfish	*unidentified*	MeOH	D
49	J-56	28	51	113	103	Sponge	*unidentified*	MeOH	D
50	J-57	8	63	94	85	Tunicate	*Pseudodistoma kanoko*	MeOH	D
51	J-58	0	2	48	65	Sponge	*unidentified*	MeOH	D
52	J-59	0	2	45	71	Sponge	*unidentified*	MeOH	D
53	J-60	98	134	122	95	Annelid	*unidentified*	MeOH	D
54	A-2	0	1	6	15	Soft coral	*Briareum*	EtOAc	A
55	A-3	0	0	6	9	Tunicate	*unidentified*	EtOAc	A
56	A-4	22	36	74	76	Sponge	*Liosina*	EtOAc	A
57	B-5	33	107	69	93	Sponge	*unidentified*	EtOAc	B
58	B-6	0	0	5	8	Sponge	*Xestospongia*	EtOAc	B
59	B-7	0	0	5	9	Sponge	*Epipolasis*	EtOAc	B
60	B-8	0	0	2	46	Sponge	*unidentified*	EtOAc	B
61	B-9	0	0	8	14	Sponge	*Strongylophora*	EtOAc	B
62	B-10	0	0	3	8	Sponge	*Stylotella aurantium*	EtOAc	B
63	C-12	0	0	4	14	Sponge	*Epipolasis*	EtOAc	B
64	C-13	0	0	4	5	Sponge	*unidentified*	EtOAc	B
65	C-14	48	119	82	102	Sponge	*Hippospongia*	EtOAc	B
66	C-15	0	0	8	11	Sponge	*unidentified*	EtOAc	B
67	C-18	0	0	4	3	Sponge	*unidentified*	EtOAc	B
68	C-19	23	76	63	109	Sponge	*unidentified*	EtOAc	B
69	C-20	34	32	63	112	Sponge	*Xestospongia testudinaria*	EtOAc	B
70	C-21	1	0	52	12	Sponge	*unidentified*	EtOAc	B
71	C-22	76	34	74	110	Sponge	*unidentified*	EtOAc	B
72	C-24	0	0	20	7	Sponge	*Theonella*	EtOAc	B
73	C-26	41	43	80	110	Sponge	*unidentified*	EtOAc	B
74	C-27	1	0	35	40	Sponge	*unidentified*	EtOAc	B
75	C-28	68	62	82	115	Sponge	*Petrosia*	EtOAc	B
76	C-29	10	11	93	88	Sponge	*Amphimedon*	EtOAc	B
77	D-31	20	71	85	120	Tunicate	*Eudistoma*	EtOAc	C
78	D-33	0	0	5	7	Gorgonian	*Junceella fragilis*	EtOAc	C
79	E-35	0	0	4	5	Sponge	*Phyllospongia sp.*	EtOAc	C
80	E-36	71	83	75	100	Tunicate	*Didemnum molle*	EtOAc	C
81	F-40	72	110	87	130	Sponge	*unidentified*	EtOAc	C
82	F-41	8	33	73	104	Soft coral	*unidentified*	EtOAc	C
83	H-43	0	197	4	119	Sponge	*unidentified*	EtOAc	D
84	J-46	113	58	103	126	Sponge	*unidentified*	EtOAc	D

There are a total of 54 marine organisms, while 84 extracts were prepared from them with ethyl acetate and/or methanol. Aragusuku, Iriomote, Kohama, and Ishigaki islands are indicated by A, B, C, and D, respectively, in the collection-site column?(right end). EtOAc: Ethyl acetate; MeOH: Methanol.

doi:10.1371/journal.pone.0048685.t001

with C-29EA inhibited dsRNA dissociation at a concentration of 16 μg/ml and above (Fig. 5B).

The unwinding ability of HCV helicase depends on ATP binding, ATP hydrolysis, and RNA binding [30,31]. We examined the effect of C-29EA on the ATPase activity of NS3. The ratio of free phosphate (^{32}P-Pi) to ATP (^{32}P-ATP) was determined in the presence of C-29EA. The reaction was carried out between 16 and 250 μg of C-29EA per milliliter. The ATPase activity of NS3 helicase was not inhibited (Fig. 6A), although the helicase activity was decreased to less than 20% in the presence of 50 μg of C-29EA per milliliter (Fig. 5A). Next, we examined the effect of C-29EA on the binding of NS3 helicase to single-strand RNA (ssRNA). A gel-mobility shift assay was employed to estimate the binding activity of NS3 to the 21-mer of ssRNA. The binding of NS3 to ssRNA was inhibited by C-29EA in a dose-dependent manner (Fig. 6 B and C). These results suggest that treatment with C-29EA inhibits the helicase activity of NS3 by suppressing RNA binding.

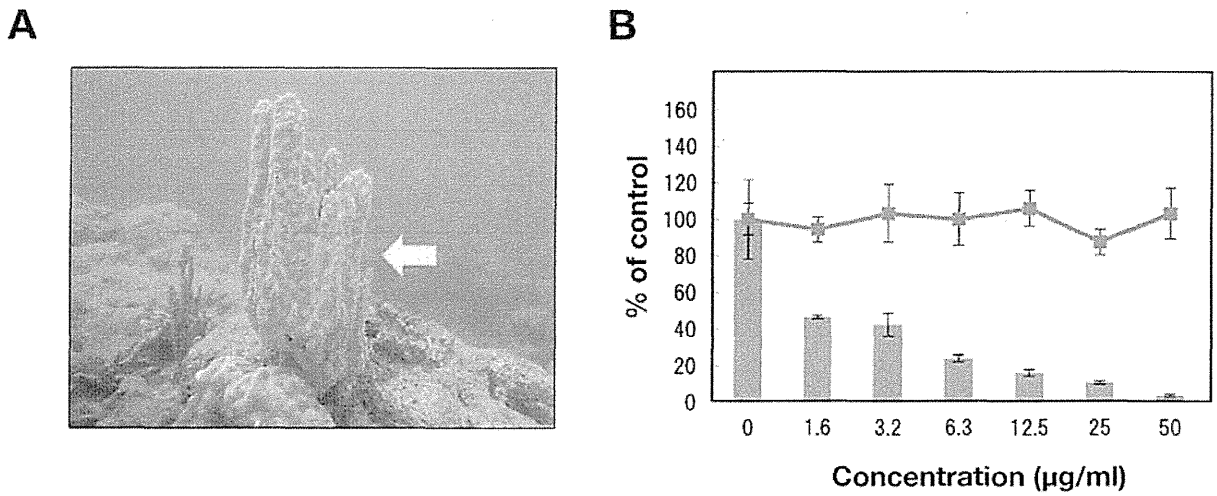

Figure 1. Effect of the extract prepared from a marine sponge on viral replication in the replicon cell line derived from viral genotype 1b. (A) *Amphimedon* sp. belongs to a marine sponge. The ethyl acetate fraction prepared from the marine organism was designated C-29EA in this study. (B) The Huh7 cell line, including the subgenomic replicon RNA of genotype 1b strain Con1, was incubated in medium containing various concentrations of C-29EA or DMSO (0). Luciferase and cytotoxicity assays were carried out as described in Materials and Methods. Error bars indicate standard deviation. The data represent three independent experiments.
doi:10.1371/journal.pone.0048685.g001

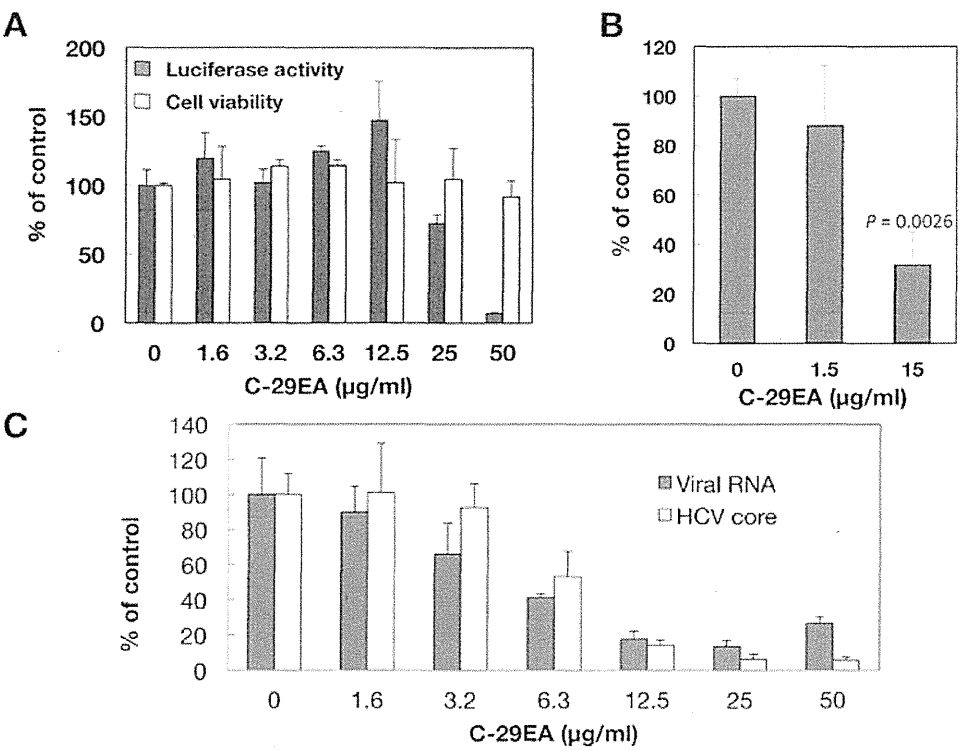

Figure 2. Effect of C-29EA extract on viral replication in the replicon cell line derived from viral genotype 2a. (A) The Huh7 cell line, including the subgenomic replicon RNA of genotype 2a strain JFH1, was incubated in medium containing various concentrations of C-29EA or DMSO (0). Luciferase and cytotoxicity assays were carried out as described in Materials and Methods. (B) The Huh7 OK1 cell line infected with HCVcc JFH1 was incubated with various concentrations of C-29EA or DMSO (0). The virus titers were determined by a focus-forming assay. The significance of differences in the means was determined by Student's *t*-test. (C) Amounts of viral RNA and core protein were estimated by qRT-PCR and ELISA, respectively. Error bars indicate standard deviation. The data represent three independent experiments. Treatment with DMSO corresponds to '0'.
doi:10.1371/journal.pone.0048685.g002

Table 2. Effect of C29EA on HCV replication.

HCV strain (genotype)	EC_{50} (μg/ml)[a]	CC_{50} (μg/ml)[b]	SI[c]
Con 1 (1b)	1.5	>50	>33.3
JFH1 (2a)	24.9	>50	>2.3

[a]: Fifty percent effective concentration based on the inhibition of HCV replication.
[b]: Fifty percent cytotoxicity concentration based on the reduction of cell viability.
[c]: SI, selectivity index (CC_{50}/EC_{50}).
doi:10.1371/journal.pone.0048685.t002

Effect of C-29EA on NS3 Protease Activity

Serine protease and helicase domains are respectively located on the N-terminal and C-terminal portions of NS3 [32]. Thus, we examined the effect of C-29EA on NS3 protease activity by using an NS3 protease assay based on FRET. NS3/4A serine protease was mixed with various concentrations of C-29EA. The initial velocity at each concentration of C-29EA was calculated during a 120 min reaction. The initial velocity in the absence of C-29EA represented 100% of relative protease activity. C-29EA decreased the serine protease activity in a dose-dependent manner (Fig. 7). The IC_{50} of C-29EA was 10.9 μg/ml, which is similar to the value estimated by helicase assay. These results suggest that C-29EA includes the compound(s) inhibiting the protease activity of NS3 in addition to the helicase activity.

Combination Antiviral Activity of C-29EA and Interferon-alpha

Treatment with C-29EA may potentiate inhibitory action of interferon-alpha, since it inhibited the protease and helicase activities of NS3 but not induce the interferon response as described above. Then, we examined effect of treatment using both interferon and C-29EA on HCV replication. The replication

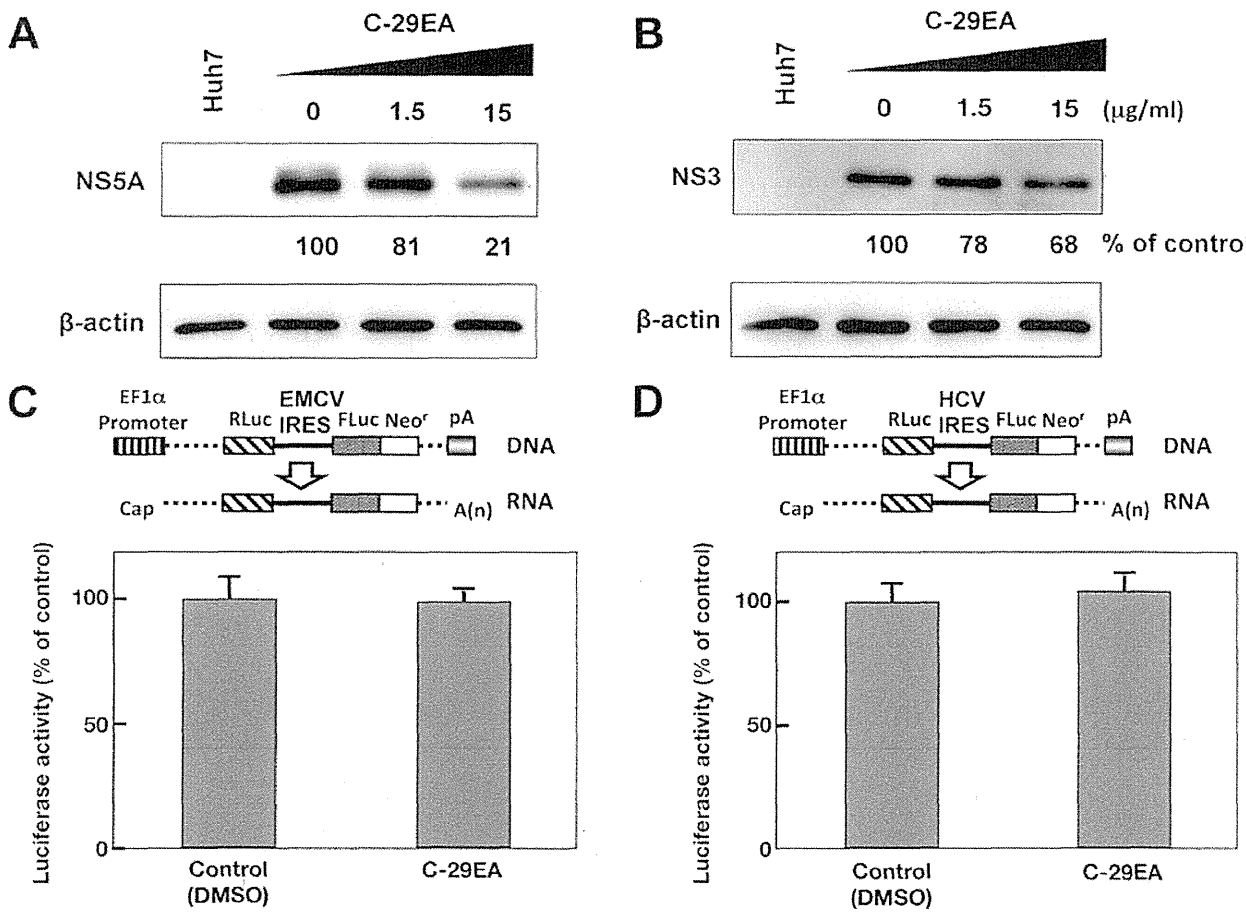

Figure 3. Effect of C-29EA on expression of viral proteins in replicon cell lines. The Huh7 replicon cell lines derived from genotype 1b (A) and 2a (B) were incubated with C-29EA at 37 C for 72 h. The treated cells were harvested and then subjected to Western blotting. Treatment with DMSO corresponds to '0'. The bicistronic gene is transcribed under the control of the elongation factor 1α (EF1α) promoter. The upstream cistron encoding *Renilla* luciferase (RLuc) is translated by a cap-dependent mechanism. The downstream cistron encodes the fusion protein (Feo), which consists of the firefly luciferase (Fluc) and neomycin phosphotransferase (Neo^r), and is translated under the control of the EMCV IRES (C) or HCV IRES (D). The Huh7 cell line transfected with the plasmid (each above the panel in C and D) was established in the presence of G418. The cells were incubated for 72 h without (control) and with 15 μg/ml of C-29EA. Firefly or *Renilla* luciferase activity was measured by the method described in Materials and Methods and was normalized by the protein concentration. F/R: relative ratio of firefly luciferase activity to *Renilla* luciferase activity. F/R is presented as a percentage of the control condition. Error bars indicate standard deviation. The data represent three independent experiments.
doi:10.1371/journal.pone.0048685.g003

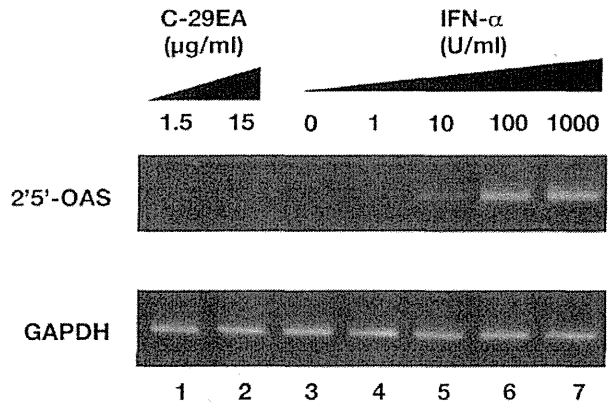

Figure 4. Effect of C-29EA on interferon signaling pathway. The Huh7 replicon cell line of genotype 1b was treated without (lane 3) or with 1, 10, 100, or 1000 U/mL interferon-alpha 2b (lanes 4–7), and 1.5 or 15 μg/ml C-29EA (lanes 1–2) for 48 h. Treatment with DMSO corresponds to '0'. The mRNAs of 2', 5'-OAS, and GAPDH as an internal control were detected by RT-PCR. Error bars indicate standard deviation. The data represent three independent experiments.
doi:10.1371/journal.pone.0048685.g004

of replicon was decreased in the presence of C-29EA or interferon-alpha and further decreased by combination treatment using interferon-alpha and C-29EA (Fig. 8A). Furthermore, we employed the isobologram method [33] to determine whether antiviral effect of the combination treatment exhibits additive or synergistic. EC_{90} values of interferon-alpha and C-29EA were estimated at 10.7 U/ml and 26.4 μg/ml, respectively, in the absence of each other. EC_{90} values of C-29EA in the presence of 0, 2.5 and 5 U/ml interferon-alpha were plotted to generate an isobole. Figure 8B shows that the isobole exhibits concave curvilinear, representing synergy but not additivity. These results suggest that combination treatment of interferon-alpha and C-29EA exhibits synergistic inhibition of HCV replication.

Discussion

Several natural products have been reported as anti-viral agents against HCV replication. Silbinin, epigallocatechin 3-gallate, and proanthocyanidins, which were prepared from milk thistle, green tea, and blueberry leaves, respectively, have exhibited inhibitory activity against HCV replication in cultured cells [34–37]. In our previous report, we identified manoalide as an anti-HCV agent from a marine sponge extract by high-throughput screening targeting NS3 helicase activity [38]. Manoalide inhibited ATPase, RNA binding, and NS3 helicase activity in enzymological assays. The EtOAc extract of the marine feather star also suppressed HCV replication in HCV replicon cell lines derived from genotype 1b, and it inhibited the RNA-binding activity but not the ATPase activity of NS3 helicase [30]. In this study, we screened 84 extracts of marine organisms for their ability to inhibit HCV replication in replicon cell lines and HCV cell culture system. Among these extracts, C-29EA, which was extracted from *Amphimedon* sp., most strongly inhibited HCV replication regardless of cytotoxicity. We previously reported that the EtOAc extract (SG1-23-1) of the feather star *Alloecomatella polycladia* inhibited HCV replication with an EC_{50} of 22.9 to 44.2 μg/ml in HCV replicon cells derived from genotype 1b [30]. Treatment with C-29EA potently inhibited HCV replication with an EC_{50} of 1.5 μg/ml and with an SI of more than 33.3 in the replicon cell line derived from genotype 1b, regardless of cytotoxicity (Fig. 1B and Table 2). However, C-29EA exhibited an EC_{50} of 24.9 μg/ml in a replicon cell line derived from genotype 2a at a weaker level than in the replicon cell line derived from genotype 1b (Figs. 1 and 2), suggesting that the ability of C-29EA to suppress HCV replication is dependent on the viral genotype or strain.

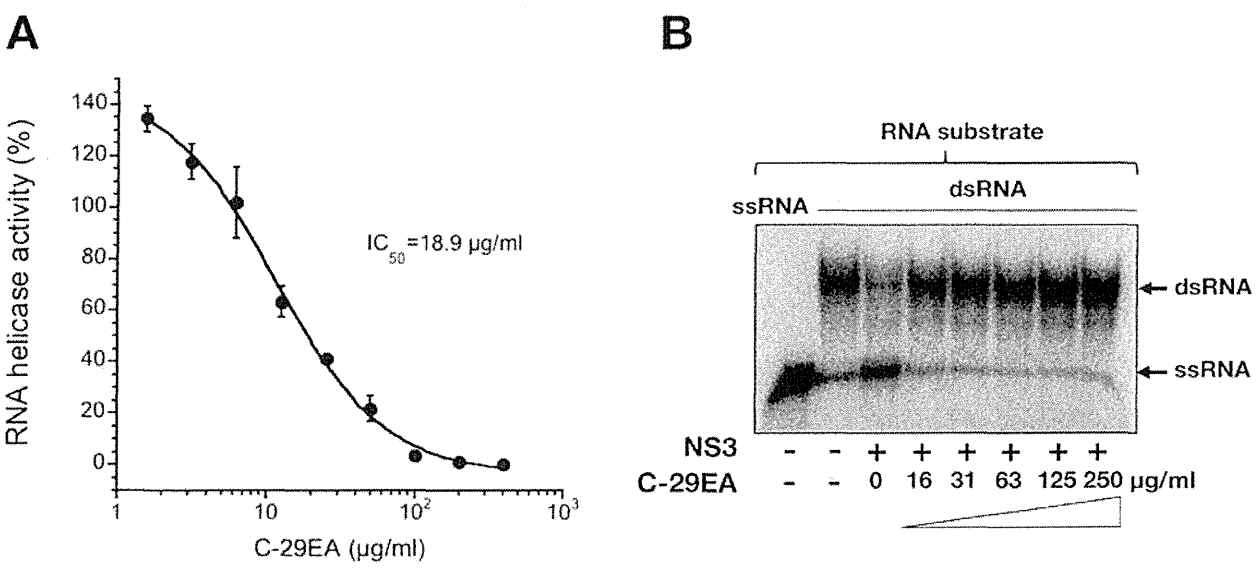

Figure 5. Effect of C-29EA on unwinding activity of NS3 helicase. (A) NS3 helicase activity was measured by PET assay. The reactions were carried out in the absence or presence of C-29EA. Helicase activity in the absence of C-29EA was defined as 100% helicase activity. Treatment with DMSO corresponds to '0'. The data are presented as the mean ± standard deviation for three replicates. (B) The unwinding activity of NS3 helicase was measured by an RNA unwinding assay using radioisotope-labeled RNA. The heat-denatured single-strand RNA (26-mer) and the partial duplex RNA substrate were applied to lanes 1 and 2, respectively. The duplex RNA was reacted with NS3 (300 nM) in the presence of C-29EA (lanes 4–9, 16–250 μg/ml). The resulting samples were subjected to native polyacrylamide gel electrophoresis. Treatment with DMSO corresponds to '0'.
doi:10.1371/journal.pone.0048685.g005

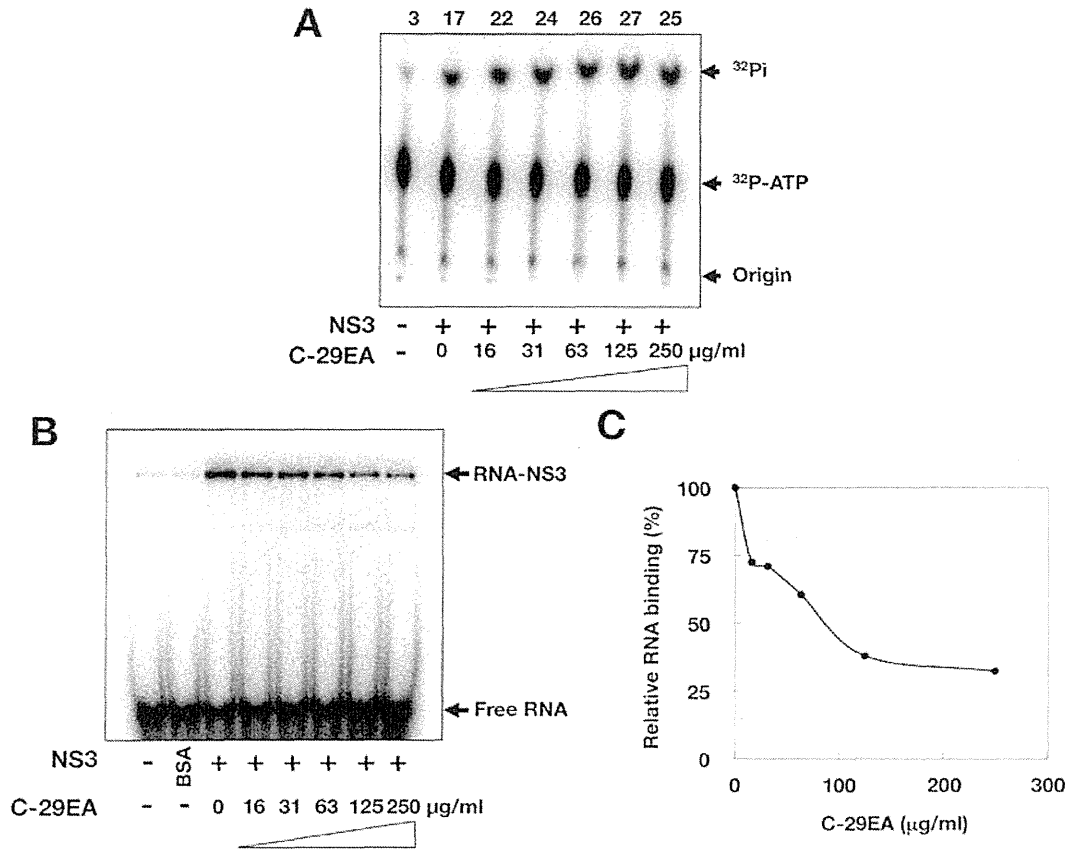

Figure 6. Effect of C-29EA on ATPase and RNA-binding activities of NS3 helicase. (A) The reaction mixtures were incubated with [γ-^{32}P] ATP as described in Materials and Methods. The reaction mixtures were subjected to thin-layer chromatography. The start positions and migrated positions of ATP and free phosphoric acid are indicated as 'Origin', '^{32}P-ATP', and '^{32}P-Pi', respectively, on the right side of the figure. The data represent three independent experiments. Treatment with DMSO corresponds to '0'. (B) Gel mobility shift assay for RNA-binding activity of NS3 helicase. The reaction was carried out with 0.5 nM labeled ssRNA at the indicated concentrations of C-29EA or DMSO. The reaction mixture was subjected to gel mobility shift assay. (C) The relative RNA-binding ability was calculated with band densities in each lane and presented as a percentage of RNA-NS3 in the total density. The data represent three independent experiments. Treatment with DMSO corresponds to '0'.
doi:10.1371/journal.pone.0048685.g006

HCV NS3 is well known to play a crucial role in viral replication through helicase and protease activities [5,39]. The N-terminal third of NS3 is responsible for serine protease activity in order to process the C-terminal portion of polyprotein containing viral nonstructural proteins [32]. The remaining portion of NS3 exhibits ATPase and RNA-binding activities responsible for helicase activity, which is involved in unwinding double-stranded RNA during replication of genomic viral RNA [40–42]. A negative-strand RNA is synthesized based on a viral genome (positive strand) after viral particles in the infected cells are uncoated, and is then used itself as a template to synthesize a positive-stranded RNA, which is translated or packaged into viral particles. Thus, both helicase and protease activities of NS3 are critical for HCV replication and could be targeted for the development of antiviral agents against HCV.

NS3 helicase activity was inhibited by treatment with C-29EA in a dose-dependent manner with an IC_{50} of 18.9 μg/ml (Fig. 5A). RNA-binding activity, but not ATPase activity, was inhibited by treatment with C-29EA (Fig. 6). Treatment with C-29EA did not significantly affect the HCV-IRES activity and did not induce interferon-stimulated gene 2′,5′-OAS (Figs. 3 and 4). Furthermore, the serine protease activity of NS3 was inhibited by using C-29EA with an IC_{50} of 10.9 μg/ml (Fig. 7). These results suggest that *Amphimedon* sp. includes the unknown compound(s) that could suppress NS3 enzymatic activity to inhibit HCV replication. Although the mechanism by which treatment with C-29EA could inhibit HCV replication has not yet been revealed, the unknown compound(s) may be associated with the inhibition of NS3 protease and helicase, leading to the suppression of HCV replication. However, other effects of extract C-29EA on HCV replication could not be excluded in this study.

The compound 1-N, 4-N-bis [4-(1H-benzimidazol-2-yl)phenyl] benzene-1,4-dicarboxamide, which is designated as $(BIP)_2B$, was reported to be a potent and selective inhibitor of HCV NS3 helicase [43]. This compound competitively decreases the binding ability of HCV NS3 helicase to nucleic acids. The compound $(BIP)_2B$ inhibited RNA-induced stimulation of ATPase, although it did not directly affect the ATP hydrolysis activity of NS3 helicase. Thus, $(BIP)_2B$ could not affect ATPase activity without RNA or with a high concentration of RNA. Treatment with C-29EA inhibited helicase activity and viral replication but not ATPase activity (Figs. 1B, 2, 5, and 6). This extract suppressed the binding of RNA to helicase but exhibited no suppression of ATPase by NS3 helicase. Thus, the inhibitory action of extract C-29EA seems

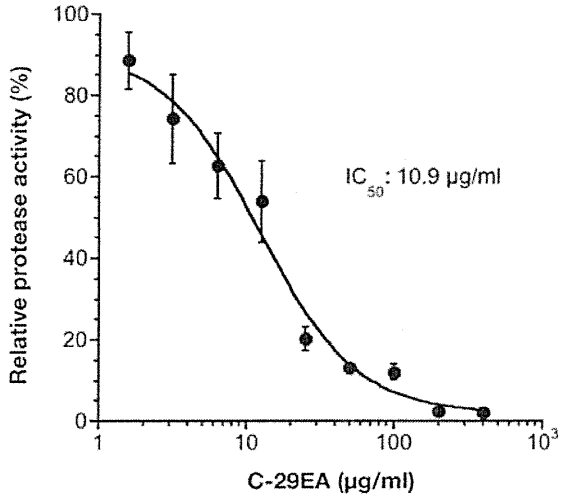

Figure 7. Effect of C-29EA on the activity of NS3 serine protease. NS3/4A serine protease was mixed with various concentrations of C-29EA or DMSO (0) in the reaction mixture and then incubated at 37°C for 120 min. The initial velocity at each concentration of C-29EA was calculated during 120 min reaction. The initial velocity in the absence of C-29EA was defined as 100% of relative protease activity. The data are presented as the mean ± standard deviation for three replicates.
doi:10.1371/journal.pone.0048685.g007

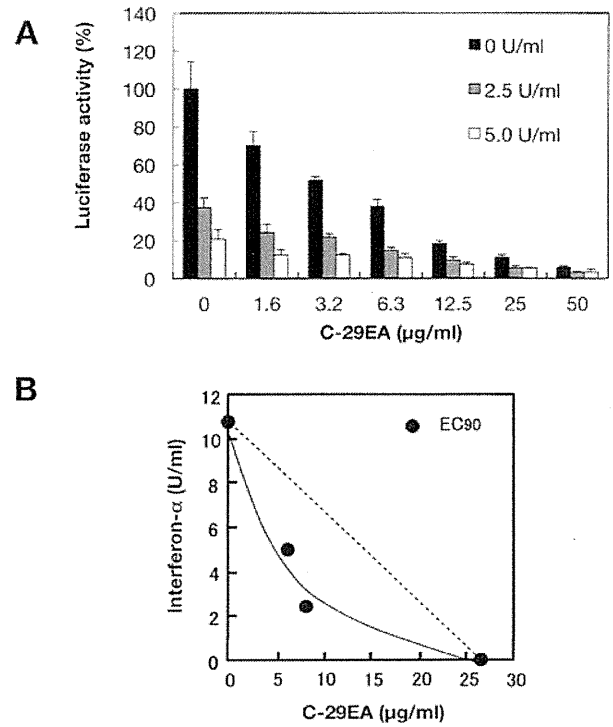

Figure 8. Effect of C-29EA on the antiviral activity of interferon-alpha. (A) The Huh7 cell line, including the subgenomic replicon RNA of genotype 1b strain Con1, was incubated in medium containing various concentrations of C-29EA or DMSO (0) in the presence or the absence of interferon-alpha. Luciferase assay were carried out as described in Materials and Methods. Error bars indicate standard deviation. The data represent three independent experiments. (B) Isobole plots of 90% inhibition of HCV replication. The broken line indicates the additive effect in the isobologram.
doi:10.1371/journal.pone.0048685.g008

different from that of $(BIP)_2B$. The quinolone derivative QU663 was reported to inhibit the unwinding activity of NS3 helicase by binding to an RNA-binding groove irrespective of its own ATPase activity [44]. The compound QU663 may competitively bind the RNA-binding site of NS3 but not affect ATPase activity, resulting in the inhibition of unwinding activity. In this study, treatment with C-29EA inhibited the RNA-binding activities of NS3 helicase but did not affect ATPase activity (Fig. 6). Furthermore, treatment with C-29EA suppressed the viral replication of HCV in an HCV cell culture system derived from several virus strains (Figs. 1 and 2, Table 2). The mechanism of C-29EA on the inhibition of NS3 helicase may be similar to that of compound QU663.

It is unknown whether one or several molecules included in C-29EA are critical for the inhibition of protease and helicase activities. The serine protease NS3/4A is one of the viral factors targeted for development into antiviral agents. Improvements in HCV therapy over the past several years have resulted in FDA approval of telaprevir (VX-950) [15,45] and boceprevir (SCH503034) [46,47]. Several studies suggest that the activities of NS3/4A protease and helicase in the full-length molecule enhance each other [48,49]. The NS3/4A protease has formed a complex with macrocyclic acylsulfonamide inhibitors [50,51]. Schiering et al. recently reported the structure of full-length NS3/4A in complex with a macrocyclic acylsulfonamide protease inhibitor [52], although the structure of full-length HCV NS3/4A in complex with a protease inhibitor has not been reported. The inhibitor binds to the active site of the protease, while the P4-capping and P2 moieties of the inhibitor are exposed toward the helicase interface and interact with both protease and helicase residues [52]. An unknown compound included in C-29EA might interact with both protease and helicase domains of NS3 to inhibit their activities. However, our data in this study have not excluded the possibility that several compounds included in C-29EA are related to the inhibition of protease and helicase of NS3/4A.

In conclusion, we showed that the EtOAc extract from *Amphimedon* sp. significantly inhibits HCV replication by suppressing viral helicase and protease activities. The purification of an inhibitory compound from the extract of *Amphimedon* sp. will be necessary in order to improve its efficacy by chemical modification.

Materials and Methods

Preparation of Extracts from Marine Organisms

All marine organisms used in this study were hand-collected by scuba diving off islands in Okinawa Prefecture, Japan. No specific permits were required for the described field studies. We do not have to obtain a local government permit to collect invertebrates except for stony corals and marine organisms for fisheries, which we did not collect in this study. The areas where we collected are not privately-owned or protected in any way. We did not collect any invertebrates listed in the red data book issued by Ministry of Environment, Japan. The sponges, tunicates, and soft corals used in this study are not listed at all. Hence, no specific permits are required for this collection in the same way as the previous report of Aratake et al. [53].

The sponge from which C-29EA was extracted was identified as *Amphimedon* sp. and deposited at Naturalis under the code RMNH POR 6100. Each specimen was soaked in acetone. The acetone-extract fraction prepared from each specimen was concentrated.

The resulting material was fractionated as an EtOAc- and water-soluble fraction. The water-soluble fraction was dried up and solubilized in MeOH. The EtOAc- and the MeOH-soluble fractions were used for screening. All samples were dried and then solubilized in dimethyl sulfoxide (DMSO) before testing.

Cell Lines and Virus

The following Huh-7-derived cell lines used in this study were maintained in Dulbecco's modified Eagle's medium containing 10% fetal calf serum and 0.5 mg/ml G418. The Lunet/Con1 LUN Sb #26 cell line, which harbors the subgenomic replicon RNA of the Con1 strain (genotype 1b), was kindly provided by Ralf Bartenschlager [26]. Huh7/ORN3-3B #24 cell line, which harbors the subgenomic replicon RNA of the O strain (genotype 1b) was reported previously [54] and used for screening in this study (Table 1). HCV replicon cell line derived from genotype 2a strain JFH1 was described previously [55]. The surviving cells were infected with the JFH-1 virus at a multiplicity of infection (moi) of 0.05. The viral RNA derived from the plasmid pJFH1 was transcribed and introduced into Huh7OK1 cells according to the method of Wakita et al. [56]. The infectivity of the JFH1 strain was determined by a focus-forming assay [56].

Quantitative Reverse-transcription PCR (qRT-PCR) and Estimation of Core Protein

The estimation of viral RNA genome was carried out by the method described previously [57] with slight modification. Total RNAs were prepared from cells and culture supernatants by using an RNeasy mini kit (QIAGEN, Tokyo, Japan) and QIAamp Viral RNA mini kit (QIAGEN), respectively. First-strand cDNA was synthesized by using a high capacity cDNA reverse transcription kit (Applied Biosystems, Carlsbad, CA, USA) with random primers. Each cDNA was estimated by using Platinum SYBR Green qPCR SuperMix UDG (Invitrogen, Carlsbad, CA, USA) according to the manufacturer's protocol. Fluorescent signals of SYBR Green were analyzed by using an ABI PRISM 7000 (Applied Biosystems). The HCV internal ribosomal entry site (IRES) region was amplified using the primer pair 5′-GAGTGTCGTGCAGCCTCCA -3′ and 5′- CACTCGCAAG-CACCCTATCA -3′. Expression of HCV core protein was determined by an enzyme-linked immunosorbent assay (ELISA) as described previously [57].

Determination of Luciferase Activity and Cytotoxicity in HCV Replicon Cells

HCV replicon cells were seeded at 2×10^4 cells per well in a 48-well plate 24 h before treatment. C-29EA was added to the culture medium at various concentrations. The treated cells were harvested 72 h post-treatment and lysed in cell culture lysis reagent (Promega, Madison, WI, USA) or *Renilla* luciferase assay lysis buffer (Promega). Luciferase activity in the harvested cells was estimated with a luciferase assay system (Promega) or a *Renilla* luciferase assay system (Promega). The resulting luminescence was detected by the Luminescencer-JNR AB-2100 (ATTO, Tokyo, Japan) and corresponded to the expression level of the HCV replicon. Cell viability was measured by a dimethylthiazol carboxymethoxy-phenylsulfophenyl tetrazolium (MTS) assay using a CellTiter 96 aqueous one-solution cell proliferation assay kit (Promega).

Effects on Activities of Internal Ribosome Entry Site (IRES)

Huh7 cells were transfected with pEF.Rluc.HCV.IRES.Fco or pEF.Rluc.EMCV.IRES.Fco and then were established in medium containing 0.25 mg/ml G418, as described previously [58]. These cell lines were seeded at 2×10^4 cells per well in a 48-well plate 24 h before treatment, treated with 15 μg/ml extract C-29EA, and then harvested at 72 h post-treatment. The firefly luciferase activities were measured with a luciferase assay system (Promega). The total protein concentration was measured using the BCA Protein Assay Reagent Kit (Thermo Scientific, Rockford, IL, USA) to normalize luciferase activity.

Western Blotting and Reverse-transcription Polymerase Chain Reaction (RT-PCR)

Western blotting was carried out by a method described previously [30]. The antibodies to NS3 (clone 8G-2, mouse monoclonal, Abcam, Cambridge, UK), NS5A (clone 256-A, mouse monoclonal, ViroGen, Watertown, MA, USA), and beta-actin were purchased from Cell Signaling Technology (rabbit polyclonal, Danvers, MA, USA) and were used as the primary antibodies in this study. RT-PCR was carried out by a method described previously [30,58].

Assays for RNA Helicase, ATPase, and RNA-binding Activities

A continuous fluorescence assay based on photoinduced electron transfer (PET) was described previously [29] and was slightly modified with regard to the reaction mixture [30]. The NS3 RNA unwinding assay was carried out by the method of Gallinari et al. [59] with slight modifications [30]. NS3 ATPase activity was determined by the method of Gallinari et al. [59] with slight modifications [30]. RNA binding to NS3 helicase was analyzed by a gel mobility shift assay [30,31]. The gene encoding NS3 helicase was amplified from the viral genome of genotype 1b and was introduced into a plasmid for the expression of a recombinant protein [38,60]. The radioactive band was visualized with the Image Reader FLA-9000 and quantified by Multi Gauge V 3.11 software.

NS3 Protease Assay

The fluorescence NS3 serine protease assay based on fluorescence resonance energy transfer (FRET) was carried out by the modified method using the SensoLyte^{TM} 520 HCV protease assay kit (AnaSpec, Fremont, CA, USA). In brief, NS3 protein with a two-fold excess of NS4A cofactor peptide (Pep4AK) was prepared in 1× assay buffer provided with the kit. HCV NS3/4A protease was mixed with increasing concentrations of C-29EA and incubated at 37°C for 15 min. The reaction was started by adding the 5-FAM/QXL 520 substrate to the reaction mixture containing 180 nM HCV NS3/4A protease and various concentrations (0–400 μg/ml) of C-29EA. The resulting mixture (20 μl) was incubated at 37°C for 120 min using a LightCycler 1.5 (Roche Diagnostics, Basel, Switzerland). The fluorescence intensity was recorded every minute for 120 min. The NS3 serine protease activity was calculated as the initial reaction velocity and presented as a percentage of relative activity to that of the control examined with DMSO solvent but not C-29EA, in the same way as described in the fluorescence helicase assay [29].

Analysis of Drug-drug Interaction

The effects of drug combinations were evaluated using the isobologram method [33]. Various doses of C-29EA and interferon-alpha on 90% inhibition of HCV replication were combined to generate an isoeffect curve (isobole) to determine drug–drug interaction. Concave, linear, and convex curves exhibit synergy, additivity, and antagonism, respectively.

Statistical Analysis

The results are expressed as the mean ± standard deviation. The significance of differences in the means was determined by Student's *t*-test.

Acknowledgments

We thank T. Wakita and R. Bartenschlager for kindly providing the virus, cell lines, and plasmids; and H. Kasai and I. Katoh for their helpful comments and discussions.

Author Contributions

Conceived and designed the experiments: MN MT YS ST NA NN AY JT KM. Performed the experiments: YF KAS AF YM OF HT AY. Analyzed the data: MI NK NS SM NE. Wrote the paper: YF AY JT KM. Collected marine organisms: JT. Identified the sponge: NJdV.

References

1. Baldo V, Baldovin T, Trivello R, Floreani A (2008) Epidemiology of HCV infection. Curr Pharm Des 14: 1646–1654.
2. Seeff LB (2002) Natural history of chronic hepatitis C. Hepatology 36: S35–46.
3. Morilishi K, Matsuura Y (2012) Exploitation of lipid components by viral and host proteins for hepatitis C virus infection. Front Microbiol 3: 54.
4. Tsukiyama-Kohara K, Iizuka N, Kohara M, Nomoto A (1992) Internal ribosome entry site within hepatitis C virus RNA. J Virol 66: 1476–1483.
5. Kim DW, Gwack Y, Han JH, Choe J (1995) C-terminal domain of the hepatitis C virus NS3 protein contains an RNA helicase activity. Biochem Biophys Res Commun 215: 160–166.
6. Kanai A, Tanabe K, Kohara M (1995) Poly(U) binding activity of hepatitis C virus NS3 protein, a putative RNA helicase. FEBS Lett 376: 221–224.
7. Manns MP, Wedemeyer H, Cornberg M (2006) Treating viral hepatitis C: efficacy, side effects, and complications. Gut 55: 1350–1359.
8. McHutchison JG, Everson GT, Gordon SC, Jacobson IM, Sulkowski M, et al. (2009) Telaprevir with peginterferon and ribavirin for chronic HCV genotype 1 infection. N Engl J Med 360: 1827–1838.
9. Zeuzem S, Hultcrantz R, Bourliere M, Goeser T, Marcellin P, et al. (2004) Peginterferon alfa-2b plus ribavirin for treatment of chronic hepatitis C in previously untreated patients infected with HCV genotypes 2 or 3. J Hepatol 40: 993–999.
10. Asselah T, Marcellin P (2011) New direct-acting antivirals' combination for the treatment of chronic hepatitis C. Liver Int 31 Suppl 1: 68–77.
11. Jazwinski AB, Muir AJ (2011) Direct-acting antiviral medications for chronic hepatitis C virus infection. Gastroenterol Hepatol (N Y) 7: 154–162.
12. Lange CM, Sarrazin C, Zeuzem S (2010) Review article: specifically targeted anti-viral therapy for hepatitis C – a new era in therapy. Aliment Pharmacol Ther 32: 14–28.
13. Hofmann WP, Zeuzem S (2011) A new standard of care for the treatment of chronic HCV infection. Nat Rev Gastroenterol Hepatol 8: 257–264.
14. Kwong AD, Kauffman RS, Hurter P, Mueller P (2011) Discovery and development of telaprevir: an NS3–4A protease inhibitor for treating genotype 1 chronic hepatitis C virus. Nat Biotechnol 29: 993–1003.
15. Jacobson IM, McHutchison JG, Dusheiko G, Di Bisceglie AM, Reddy KR, et al. (2011) Telaprevir for previously untreated chronic hepatitis C virus infection. N Engl J Med 364: 2405–2416.
16. Sarrazin C, Hezode C, Zeuzem S, Pawlotsky JM (2012) Antiviral strategies in hepatitis C virus infection. J Hepatol 56 Suppl 1: S88–100.
17. Chen ST, Wu PA (2012) Severe Cutaneous Eruptions on Telaprevir. J Hepatol 57: 470–472.
18. Kieffer TL, Kwong AD, Picchio GR (2010) Viral resistance to specifically targeted antiviral therapies for hepatitis C (STAT-Cs). J Antimicrob Chemother 65: 202–212.
19. Thompson AJ, McHutchison JG (2009) Antiviral resistance and specifically targeted therapy for HCV (STAT-C). J Viral Hepat 16: 377–387.
20. Chin YW, Balunas MJ, Chai HB, Kinghorn AD (2006) Drug discovery from natural sources. AAPS J 8: E239–253.
21. Koehn FE, Carter GT (2005) The evolving role of natural products in drug discovery. Nat Rev Drug Discov 4: 206–220.
22. Li JW, Vederas JC (2009) Drug discovery and natural products: end of an era or an endless frontier? Science 325: 161–165.
23. Donia M, Hamann MT (2003) Marine natural products and their potential applications as anti-infective agents. Lancet Infect Dis 3: 338–348.
24. Molinski TF, Dalisay DS, Lievens SL, Saludes JP (2009) Drug development from marine natural products. Nat Rev Drug Discov 8: 69–85.
25. Mayer AM, Glaser KB, Cuevas C, Jacobs RS, Kem W, et al. (2010) The odyssey of marine pharmaceuticals: a current pipeline perspective. Trends Pharmacol Sci 31: 255–265.
26. Frese M, Barth K, Kaul A, Lohmann V, Schwarzle V, et al. (2003) Hepatitis C virus RNA replication is resistant to tumour necrosis factor-alpha. J Gen Virol 84: 1253–1259.
27. Blight KJ, Kolykhalov AA, Rice CM (2000) Efficient initiation of HCV RNA replication in cell culture. Science 290: 1972–1974.
28. Guo JT, Bichko VV, Seeger C (2001) Effect of alpha interferon on the hepatitis C virus replicon. J Virol 75: 8516–8523.
29. Tani H, Akimitsu N, Fujita O, Matsuda Y, Miyata R, et al. (2009) High-throughput screening assay of hepatitis C virus helicase inhibitors using fluorescence-quenching phenomenon. Biochem Biophys Res Commun 379: 1054–1059.
30. Yamashita A, Salam KA, Furuta A, Matsuda Y, Fujita O, et al. (2012) Inhibition of hepatitis C virus replication and NS3 helicase by the extract of the feather star *Alloeocomatella polycladia*. Mar Drugs 10: 744–761.
31. Huang Y, Liu ZR (2002) The ATPase, RNA unwinding, and RNA binding activities of recombinant p68 RNA helicase. J Biol Chem 277: 12810–12815.
32. Failla C, Tomei L, De Francesco R (1994) Both NS3 and NS4A are required for proteolytic processing of hepatitis C virus nonstructural proteins. J Virol 68: 3753–3760.
33. Leu GZ, Lin TY, Hsu JT (2004) Anti-HCV activities of selective polyunsaturated fatty acids. Biochem Biophys Res Commun 318: 275–280.
34. Ahmed-Belkacem A, Ahnou N, Barbotte L, Wychowski C, Pallier C, et al. (2010) Silibinin and related compounds are direct inhibitors of hepatitis C virus RNA-dependent RNA polymerase. Gastroenterology 138: 1112–1122.
35. Ciesek S, von Hahn T, Colpitts CC, Schang LM, Friesland M, et al. (2011) The green tea polyphenol, epigallocatechin-3-gallate, inhibits hepatitis C virus entry. Hepatology 54: 1947–1955.
36. Takeshita M, Ishida Y, Akamatsu E, Ohmori Y, Sudoh M, et al. (2009) Proanthocyanidin from blueberry leaves suppresses expression of subgenomic hepatitis C virus RNA. J Biol Chem 284: 21165–21176.
37. Wagoner J, Negash A, Kane OJ, Martinez LE, Nahmias Y, et al. (2010) Multiple effects of silymarin on the hepatitis C virus lifecycle. Hepatology 51: 1912–1921.
38. Salam KA, Furuta A, Noda N, Tsuneda S, Sekiguchi Y, et al. (2012) Inhibition of Hepatitis C Virus NS3 Helicase by Manoalide. J Nat Prod 75: 650–654.
39. Bartenschlager R, Ahlborn-Laake L, Mous J, Jacobsen H (1993) Nonstructural protein 3 of the hepatitis C virus encodes a serine-type proteinase required for cleavage at the NS3/4 and NS4/5 junctions. J Virol 67: 3835–3844.
40. Belon CA, Frick DN (2009) Helicase inhibitors as specifically targeted antiviral therapy for hepatitis C. Future Virol 4: 277–293.
41. Frick DN (2007) The hepatitis C virus NS3 protein: a model RNA helicase and potential drug target. Curr Issues Mol Biol 9: 1–20.
42. Kwong AD, Rao BG, Jeang KT (2005) Viral and cellular RNA helicases as antiviral targets. Nat Rev Drug Discov 4: 845–853.
43. Belon CA, High YD, Lin TI, Pauwels F, Frick DN (2010) Mechanism and specificity of a symmetrical benzimidazolephenylcarboxamide helicase inhibitor. Biochemistry 49: 1822–1832.
44. Maga G, Gemma S, Fattorusso C, Locatelli GA, Butini S, et al. (2005) Specific targeting of hepatitis C virus NS3 RNA helicase. Discovery of the potent and selective competitive nucleotide-mimicking inhibitor QU663. Biochemistry 44: 9637–9644.
45. Reesink HW, Zeuzem S, Weegink CJ, Forestier N, van Vliet A, et al. (2006) Rapid decline of viral RNA in hepatitis C patients treated with VX-950: a phase Ib, placebo-controlled, randomized study. Gastroenterology 131: 997–1002.
46. Malcolm BA, Liu R, Lahser F, Agrawal S, Belanger B, et al. (2006) SCH 503034, a mechanism-based inhibitor of hepatitis C virus NS3 protease, suppresses polyprotein maturation and enhances the antiviral activity of alpha interferon in replicon cells. Antimicrob Agents Chemother 50: 1013–1020.
47. Njoroge FG, Chen KX, Shih NY, Piwinski JJ (2008) Challenges in modern drug discovery: a case study of boceprevir, an HCV protease inhibitor for the treatment of hepatitis C virus infection. Acc Chem Res 41: 50–59.
48. Beran RK, Pyle AM (2008) Hepatitis C viral NS3–4A protease activity is enhanced by the NS3 helicase. J Biol Chem 283: 29929–29937.
49. Beran RK, Serebrov V, Pyle AM (2007) The serine protease domain of hepatitis C viral NS3 activates RNA helicase activity by promoting the binding of RNA substrate. J Biol Chem 282: 34913–34920.
50. Cummings MD, Lindberg J, Lin TI, de Kock H, Lenz O, et al. (2010) Induced-fit binding of the macrocyclic noncovalent inhibitor TMC435 to its HCV NS3/NS4A protease target. Angew Chem Int Ed Engl 49: 1652–1655.
51. Romano KP, Ali A, Royer WE, Schiffer CA (2010) Drug resistance against HCV NS3/4A inhibitors is defined by the balance of substrate recognition versus inhibitor binding. Proc Natl Acad Sci U S A 107: 20986–20991.
52. Schiering N, D'Arcy A, Villard F, Simic O, Kamke M, et al. (2011) A macrocyclic HCV NS3/4A protease inhibitor interacts with protease and helicase residues in the complex with its full-length target. Proc Natl Acad Sci U S A 108: 21052–21056.

53. Aratake S, Tomura T, Saitoh S, Yokokura R, Kawanishi Y, et al. (2012) Soft coral Sarcophyton (Cnidaria: Anthozoa: Octocorallia) species diversity and chemotypes. PLoS One 7: e30410.
54. Ikeda M, Abe K, Dansako H, Nakamura T, Naka K, et al. (2005) Efficient replication of a full-length hepatitis C virus genome, strain O, in cell culture, and development of a luciferase reporter system. Biochem Biophys Res Commun 329: 1350–1359.
55. Nishimura-Sakurai Y, Sakamoto N, Mogushi K, Nagaie S, Nakagawa M, et al. (2010) Comparison of HCV-associated gene expression and cell signaling pathways in cells with or without HCV replicon and in replicon-cured cells. J Gastroenterol 45: 523–536.
56. Wakita T, Pietschmann T, Kato T, Date T, Miyamoto M, et al. (2005) Production of infectious hepatitis C virus in tissue culture from a cloned viral genome. Nat Med 11: 791–796.
57. Moriishi K, Shoji I, Mori Y, Suzuki R, Suzuki T, et al. (2010) Involvement of PA28gamma in the propagation of hepatitis C virus. Hepatology 52: 411–420.
58. Jin H, Yamashita A, Mackawa S, Yang P, He L, et al. (2008) Griseofulvin, an oral antifungal agent, suppresses hepatitis C virus replication in vitro. Hepatol Res 38: 909–918.
59. Gallinari P, Brennan D, Nardi C, Brunetti M, Tomei L, et al. (1998) Multiple enzymatic activities associated with recombinant NS3 protein of hepatitis C virus. J Virol 72: 6758–6769.
60. Nishikawa F, Funaji K, Fukuda K, Nishikawa S (2004) In vitro selection of RNA aptamers against the HCV NS3 helicase domain. Oligonucleotides 14: 114–129.

Journal of proteome research

Article

pubs.acs.org/jpr

Proteomic Analysis of Hepatitis C Virus (HCV) Core Protein Transfection and Host Regulator PA28γ Knockout in HCV Pathogenesis: A Network-Based Study

Lokesh P. Tripathi,[†,∥] Hiroto Kambara,[‡,∥] Kohji Moriishi,[‡] Eiji Morita,[‡] Takayuki Abe,[‡] Yoshio Mori,[‡] Yi-An Chen,[†,§] Yoshiharu Matsuura,[‡] and Kenji Mizuguchi*[,†,§]

[†]National Institute of Biomedical Innovation, 7-6-8 Saito Asagi, Ibaraki, Osaka, 567-0085, Japan

[‡]Department of Molecular Virology, Research Institute for Microbial Diseases and [§]Graduate School of Frontier Biosciences, Osaka University, 3-1 Yamada-Oka, Suita, Osaka, 565-0871, Japan

Supporting Information

ABSTRACT: Hepatitis C virus (HCV) causes chronic liver disease worldwide. HCV Core protein (Core) forms the viral capsid and is crucial for HCV pathogenesis and HCV-induced hepatocellular carcinoma, through its interaction with the host factor proteasome activator PA28γ. Here, using BD-PowerBlot high-throughput Western array, we attempt to further investigate HCV pathogenesis by comparing the protein levels in liver samples from Core-transgenic mice with or without the knockout of PA28γ expression (abbreviated PA28γ$^{-/-}$CoreTG and CoreTG, respectively) against the wild-type (WT). The differentially expressed proteins integrated into the human interactome were shown to participate in compact and well-connected cellular networks. Functional analysis of the interaction networks using a newly developed data warehouse system highlighted cellular pathways associated with vesicular transport, immune system, cellular adhesion, and cell growth and death among others that were prominently influenced by Core and PA28γ in HCV infection. Follow-up assays with *in vitro* HCV cell culture systems validated VTI1A, a vesicular transport associated factor, which was upregulated in CoreTG but not in PA28γ$^{-/-}$CoreTG, as a novel regulator of HCV release but not replication. Our analysis provided novel insights into the Core-PA28γ interplay in HCV pathogenesis and identified potential targets for better anti-HCV therapy and potentially novel biomarkers of HCV infection.

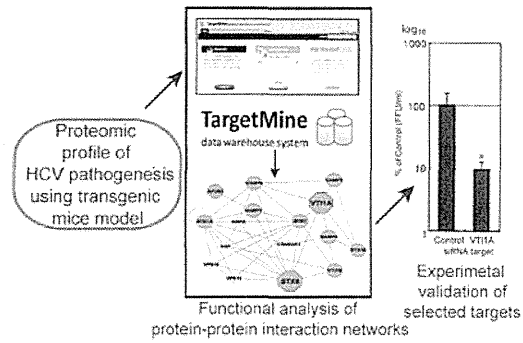

KEYWORDS: *CoreTG, GO, HCC, HCV, KEGG, OMIM, PA28γ$^{-/-}$CoreTG, PPI, siRNA, TargetMine*

INTRODUCTION

Hepatitis C virus (HCV) is a prime cause of chronic liver disease frequently characterized by liver inflammation with accompanying steatosis, progressive fibrosis, and hepatocellular carcinoma (HCC) and infects nearly 3% of the world's population. HCV contains a single-stranded RNA genome encoding a 3000-amino-acid polyprotein, which is processed by host and viral factors to yield 10 viral proteins, Core, E1, E2, p7, NS2, NS3, NS4A, NS4B, NS5A, and NS5B.[1−4] HCV variants are classified into six major genotypes with multiple subtypes characterized by phylogenetic heterogeneity, differences in infectivity, and interferon sensitivity.[5,6] The availability of cell-culture-based systems for HCV infection has provided an increased understanding of HCV pathogenesis.[5,7−9] Transgenic mice (preferably C57BL strain) expressing HCV proteins in the liver are also a preferred choice for the investigation of HCV pathogenesis.[10] However, despite considerable research efforts, precise molecular mechanisms underlying HCV pathology remain unclear.

HCV Core protein (hereafter referred to as Core) is spliced from the polyprotein by the signal peptidase and further processed into a highly conserved 21-kDa mature form by the signal peptide peptidase; this processing facilitates its transfer to the detergent-resistant membrane fraction where virus replication and assembly take place. Core is a multifunctional protein implicated in RNA binding and as a pathogenic factor; it induces steatosis and HCC and, thus, liver failure.[1,10] The ubiquitin-proteasome pathway, the premier intracellular protein degradation system in eukaryotes, is a key regulator of cellular processes and is also associated with the evasion of host immune response by many viruses, viral maturation, and progeny release.[11] Core binds to the proteasome activator PA28γ in the nucleus and is degraded via a PA28γ-dependent pathway. PA28γ plays a crucial role in Core-induced insulin resistance, steatogenesis, and hepatocarcinogenesis and in HCV propagation; PA28γ knockout in Core transgenic mice disrupts

Received: February 7, 2012
Published: May 31, 2012

steatosis and HCC, restores insulin sensitivity, and impairs viral particle production, and thus PA28γ is a promising target for anti-HCV therapies with minimal side effects.[2,12−15] However, the exact mechanisms through which PA28γ facilitates Core-induced HCV pathogenesis remain poorly understood.

In this study, we aim to put forth biological networks that describe the differential expression of the host proteins and their likely roles in modulating PA28γ function in HCV pathogenesis. We employed PowerBlot Western Array screening system, a high-throughput Western blotting method, to identify changes at the proteome level in Core expressing transgenic C57BL/6 mice with or without the knockout of PA28γ gene expression (abbreviated PA28$\gamma^{-/-}$CoreTG and CoreTG, respectively). In our analysis, we included human protein interaction data and gene regulatory information for the differentially expressed proteins using TargetMine, an integrated data warehouse that we have developed recently.[16] Our network-based analyses of the proteomic changes from the three data sets (CoreTGvsC57BL/6, PA28$\gamma^{-/-}$CoreTGvsC57BL/6 and PA28$\gamma^{-/-}$CoreTGvsCoreTG) provided novel insights into PA28γ function in Core-induced HCV pathogenesis. Furthermore, we identified VTI1A, a vesicular transport associated factor, which was upregulated in CoreTG but not in PA28$\gamma^{-/-}$CoreTG, as a novel regulator of HCV release and, thus, an attractive target for anti-HCV therapy.

MATERIALS AND METHODS

Protein Sample Preparation

Protein samples were prepared from the livers of the C57BL/6 wild-type (hereafter referred to as WT) and the transgenic mice expressing HCV Core protein genotype 1b line C49 with (PA28$\gamma^{-/-}$CoreTG) or without (CoreTG) the knockout of PA28γ expression.[2,12] Livers were harvested from three individuals each of WT, CoreTG, and PA28$\gamma^{-/-}$CoreTG mice, and the harvested samples for each mice type were pooled together prior to protein sample preparation for PowerBlot analysis. The pooled liver samples of each mice type were homogenized in 1x sample buffer of SDS-PAGE on ice and then boiled for 5 min. The boiled sample was sonicated for the viscosity of DNA and employed for PowerBlot analysis.

PowerBlot Western Array Analysis

The levels of differentially expressed proteins were determined by the PowerBlot assay by BD Biosciences Pharmingen (San Diego, CA, USA). Briefly, samples containing 200 μg of protein was loaded in one big well on top of a 4−15% gradient SDS-polyacrylamide gel and separated by electrophoresis (1.5 h at 150v). The proteins were transferred to Immobilon-FL membrane (Millipore, Billerica, MA, USA) for 2 h at 200 mA. After transfer, the membranes were incubated in the blocking buffer (LI-COR, Lincoln, NE, USA). The membrane was clamped with a Western blotting manifold that isolates 41 channels across the membrane. Each channel was incubated with a complex antibody cocktail for 1 h. The blots were removed from the manifold, washed, and hybridized for 30 min with secondary goat anti-mouse antibody conjugated to Alexa680 fluorescent dye (Molecular Probes, Eugene, OR, USA). Image data were captured using the Odyssey Infrared Imaging System (LI-COR). Data analysis included the raw and normalized signal intensity data from each blot. The results were expressed as fold change that represented the protein changes, either increasing or decreasing in the comparative analysis between the experimental samples and the control. The detected protein expression changes were listed in the order of confidence, 0 through 3, with 3 being the highest level of confidence, based on the signal quality. Only the data from confidence levels 2 and 3 (good quality signals; Supporting Information; Tables S1, S2a, S2b, and S2c) for proteins mapped to valid accessions were considered for further analysis. Proteins that displayed >1.8-fold change in abundance were judged to be differentially expressed, following the manufacturer's recommendation.

Human Orthologues for the Differentially Expressed Proteins

BD PowerBlot assay employs a cocktail of monoclonal antibodies that target human, mouse, and rat proteins, and in a specific study, over 90% were found to cross-react with proteins from human, mouse and rat[17] (Table S1). Human orthologues for the proteins picked up by the antibody cocktail were retrieved from KEGG (Tables S2a, S2b, and S2c).

Construction of Protein−Protein Interaction Networks

PPIs for the human orthologues of each set of differentially expressed proteins were retrieved from BioGRID 3.1.74[18] and iRefIndex 8.0[19] databases along with the interactions between the primary interactors of the differentially expressed proteins using TargetMine.[16] TargetMine is an integrated data warehouse that combines different biological data types and employs an objective protocol to prioritize candidate genes for further experimental investigation.[16] The interactions were merged and filtered for redundancy to infer overall extended PPI networks. Protein identifiers used in the different databases were mapped to Entrez gene IDs and official gene symbols. The official gene symbols are used hereafter, to refer to the differentially expressed proteins (Table 1) and their interacting partners. All the relationships discussed should be interpreted as protein relationships unless otherwise clarified.

PPI Network Topological Analysis

Network components were visualized using Cytoscape 2.6,[20] while network properties such as *node degree distribution* and *shortest path* measures were computed using the Cytoscape NetworkAnalyzer plugin[21] as described previously.[22] In a PPI network, the degree of a node (protein) is defined as the number of nodes directly connected to (interacting with) it, i.e., its first neighbors. *Node degree distribution*, $P(k)$, is the number of nodes with a degree k for $k = 0, 1, 2, \ldots$. The *shortest path length* between two nodes n and m, $L(n,m)$, is the minimal number of interactions that link proteins n and m in a PPI network. The *shortest path length distribution* is the number of node pairs (n,m) with $L(n,m) = x$ for $x = 1, 2, \ldots$. The *average shortest path length*, also known as the *characteristic path length*, gives the expected distance between two connected nodes i.e. the minimal number of interactions that link any two proteins in a PPI network.

Functional Analysis by Characterization of Enriched Biological Associations

Gene ontology (GO) associations retrieved from GO consortium,[23] biological pathway data from KEGG (retrieved on March 1, 2011),[24] and disease phenotype associations from OMIM[25] were used to assign functional annotations to the constituents of the extended PPI networks. The proteins in each of the extended PPI networks were uploaded to TargetMine to create protein lists, and the enrichment of specific biological themes (GO terms, KEGG Pathways, OMIM phenotypes) associated with each PPI network was estimated

dx.doi.org/10.1021/pr300121a | J. Proteome Res. 2012, 11, 3664−3679

Table 1. Summary of PowerBlot Detected Protein Expression Levels in Protein Samples

CoreTGvsWT

protein	gene ID	symbol	confidence level[a]	(−) under, (+) over[b]	fold change[c]
P31749	207	AKT1	3	−	2.68
P07355	302	ANXA2	3	+	2.92
O43747	164	AP1G1	3	+	5.72
P63010	163	AP2B1	3	+	2.40
Q96CW1	1173	AP2M1	2	+	1.93
Q9Y2T2	26985	AP3M1	2	+	1.89
P05089	383	ARG1	2	+	2.08
P52566	397	ARHGDIB	3	+	2.02
O15145	10094	ARPC3	2	−	2.25
P49407	408	ARRB1	3	−	2.33
Q07812	581	BAX	3	+	2.03
P55212	839	CASP6	3	−	1.95
Q14790	841	CASP8	2	+	2.18
Q03135	857	CAV1	2	+	2.07
P12830	999	CDH1	3	−	2.33
P19022	1000	CDH2	3	+	4.57
Q53SH4	1134	CHRNA1	3	−	3.11
P21964	1312	COMT	2	+	2.96
P00450	1356	CP	3	+	2.36
P21291	1465	CSRP1	3	+	2.23
P49711	10664	CTCF	3	+	6.13
P25685	3337	DNAJB1	3	−	2.16
P63241	1984	EIF5A	3	+	1.94
P42566	2060	EPS15	3	+	4.28
Q92889	2072	ERCC4	3	+	5.43
O75899	9568	GABBR2	3	+	3.39
O43719	27336	HTATSF1	3	+	5.76
P06756	3685	ITGAV	3	+	6.32
Q14974	3837	KPNB1	3	−	1.86
Q16539	1432	MAPK14	3	−	2.81
Q9UPY8	22924	MAPRE3	3	+	2.46
P49736	4171	MCM2	3	+	1.87
P62166	23413	NCS1	3	−	2.24
Q8IZS7	140767	NRSN1	3	+	1.89
Q16620	4915	NTRK2	3	+	2.40
Q14980	4926	NUMA1	3	−	1.94
P07237	5034	P4HB	3	+	2.27
Q92878	10111	RAD50	3	+	4.93
Q99638	5883	RAD9A	2	−	3.10
P20936	5921	RASA1	3	+	1.86
Q96SB4	6732	SRPK1	3	+	3.11
Q92186	8128	ST8SIA2	3	+	5.11
P42224	6772	STAT1	3	+	2.00
P40763	6774	STAT3	3	+	2.30
Q9UNK0	9482	STX8	3	+	1.88
Q12800	7024	TFCP2	3	+	5.04
Q92752	7143	TNR	3	+	5.36
Q13263	10155	TRIM28	3	+	4.70
O43396	9352	TXNL1	3	−	4.82
P50552	7408	VASP	2	−	2.61
Q96AJ9	143187	VTI1A	3	+	3.25
Q14191	7486	WRN	3	+	17.12

altered protein levels in PA28γ⁻/⁻CoreTGvsWT

protein	gene ID	symbol	confidence level[a]	(−) under, (+) over[b]	fold change[c]
O15145	10094	ARPC3	2	−	1.96
P49407	408	ARRB1	3	−	2.17
P55212	839	CASP6	3	−	2.04

altered protein levels in PA28γ⁻/⁻CoreTGvsWT

protein	gene ID	symbol	confidence level[a]	(−) under, (+) over[b]	fold change[c]
O60508	51362	CDC40	2	+	1.99
P54105	1207	CLNS1A	3	+	2.41
P21964	1312	COMT	2	+	2.71
P67870	1460	CSNK2B	3	+	1.90
P78352	1742	DLG4	2	+	4.08
Q95GK7	1837	DTNA	3	−	2.42
P55010	1983	EIF5	3	+	2.19
Q08495	2039	EPB49	3	+	2.66
P37268	2222	FDFT1	2	+	5.68
P09038	2247	FGF2	2	+	2.69
P62962	2280	FKBP1A	2	+	1.89
O75146	9026	HIP1R	2	−	2.08
Q9NZL4	23640	HSPBP1	3	+	3.46
P05412	3725	JUN	2	+	2.15
P52292	3838	KPNA2	3	−	7.28
P36507	5605	MAP2K2	3	−	2.35
Q16539	1432	MAPK14	3	−	3.29
P22033	4594	MUT	3	+	2.46
P54920	8775	NAPA	2	−	1.97
Q8IZS7	140767	NRSN1	3	+	1.93
Q16620	4915	NTRK2	3	+	2.50
P07237	5034	P4HB	3	+	2.04
Q08209	5530	PPP3CA	3	+	7.55
Q06124	5781	PTPN11	2	+	2.33
Q99638	5883	RAD9A	2	−	1.97
P43487	5902	RANBP1	3	+	2.29
Q9UPX8	22941	SHANK2	3	−	1.94
P29353	6464	SHC1	3	+	3.27
Q92186	8128	ST8SIA2	3	+	4.06
P31948	10963	STIP1	3	−	1.99
O75558	8676	STX11	2	+	2.04
P23193	6917	TCEA1	3	−	2.17
P07101	7054	TH	2	+	2.78
P13693	7178	TPT1	3	−	1.93
Q15628	8717	TRADD	3	−	2.00
P50607	7275	TUB	3	+	1.91

altered protein levels in PA28γ⁻/⁻CoreTGvsCoreTG

protein	gene ID	symbol	confidence level[a]	(−) under, (+) over[b]	fold change[c]
P07355	302	ANXA2	3	−	2.96
O43747	164	AP1G1	3	−	4.20
P63010	163	AP2B1	3	−	3.01
Q96CW1	1173	AP2M1	2	−	1.88
Q9Y2T2	26985	AP3M1	3	+	2.38
O00499	274	BIN1	2	−	1.88
Q9UQM7	815	CAM2KA	3	+	2.06
Q8N5S9	84254	CAMKK1	2	+	5.78
P19022	1000	CDH2	3	−	3.85
P25108	1134	CHRNA1	3	+	2.55
P49674	1454	CSNK1E	3	+	1.97
P67870	1460	CSNK2B	3	+	1.88
P21291	1465	CSRP1	3	+	1.87
P49711	10664	CTCF	3	−	5.43
Q8WTW3	9382	COG1	3	−	7.02
P00450	1356	CP	3	−	3.55
Q13618	8452	CUL3	3	+	1.91
P78352	1742	DLG4	2	+	2.13
Q9Y4J8	1837	DTNA	3	−	2.94

dx.doi.org/10.1021/pr300121a | J. Proteome Res. 2012, 11, 3664−3679

Table 1. continued

altered protein levels in PA28γ⁻/⁻CoreTGvsCoreTG					
protein	gene ID	symbol	confidence level[a]	(−) under, (+) over[b]	fold change[c]
Q08495	2039	EBP49	3	+	2.30
O14682	8507	ENC1	3	+	2.88
P42566	2060	EPS15	3	−	2.11
Q92889	2072	ERCC4	3	−	3.49
P09038	2247	FGF2	2	−	2.18
P62962	2280	FKBP1A	2	+	2.59
P49356	2342	FNTB	2	+	1.95
O75899	9568	GABBR2	3	−	2.53
O75146	9026	HIP1R	3	−	1.97
Q9NZL4	23640	HSPBP1	3	+	3.60
P61604	3336	HSPE1	3	−	2.17
Q99730	27336	HTATSF1	3	−	9.24
Q9Y6K9	8517	IKBKG	2	+	1.97
P52292	3838	KPNA2	3	−	3.94
P36507	5605	MAP2K2	3	−	2.66
Q13505	4580	MTX1	3	−	1.90
P62166	23413	NCS1	3	+	2.56
Q14980	4926	NUMA1	2	+	1.87
P41236	5504	PPP1R2	3	−	2.25
Q08209	5530	PPP3CA	3	+	12.94
P13861	5576	PRKAR2A	3	−	1.88
Q15276	9135	RABEP1	2	−	2.74

altered protein levels in PA28γ⁻/⁻CoreTGvsCoreTG					
protein	gene ID	symbol	confidence level[a]	(−) under, (+) over[b]	fold change[c]
Q92878	10111	RAD50	3	−	5.19
P20936	5921	RASA1	3	+	2.50
P06400	5925	RB1	3	+	2.50
Q92854	10507	SEMA4D	2	+	2.00
Q92529	53358	SHC3	3	−	1.90
P63208	6500	SKP1	3	−	2.45
P43004	6506	SLC1A2	2	+	2.27
Q4U2R8	9356	SLC22A6	3	−	2.23
P42224	6772	STAT1	3	−	1.90
P31948	10963	STIP1	3	−	1.98
O75558	8676	STX11	2	+	3.52
Q8IZU3	50511	SYCP3	3	+	1.88
P07101	7054	TH	2	+	2.62
Q92752	7143	TNR	3	−	4.62
O43396	9352	TXNL1	2	+	3.05
P13693	7178	TPT1	3	−	2.85
Q13263	10155	TRIM28	3	−	3.53
Q15628	8717	TRADD	3	−	2.98
P50607	7275	TUB	3	+	1.96
P41542	8615	USO1	3	−	2.05
Q14191	7486	WRN	3	−	3.44

[a]Defined as follows: Level 3 = changes greater than 2-fold from good quality signals that also pass a visual inspection. Level 2 = changes greater than 2-fold from good quality signals that do not pass a visual inspection. [b]+ indicates an increase in protein level in the experimental sample relative to control. − indicates a decrease in protein level in the experimental sample relative to control. [c]A semiquantitative value that represents the general trend of protein changes for the experimental sample relative to control.

by performing the hypergeometric test within TargetMine.[16] The inferred p-values were further adjusted for multiple test correction to control the false discovery rate using the Benjamini and Hochberg procedure,[26,27] and the annotations/pathways were considered significant if $p \leq 0.05$.

Transcription Factor-Target Associations

Transcription factor (TF)-target associations for the differentially expressed proteins were retrieved from the TF-target repository compiled from Amadeus[28] and ORegAnno[29] in TargetMine[16] and are discussed in the Supporting Information.

RNAi and Transfection

The siRNA pair targets to VTI1A, STX8, and COMT were purchased from Ambion (Ambion, Austin, TX, USA). Stealth RNAi Negative Control Low GC Duplex (Invitrogen, Carlsbad, CA, USA) was used as a control siRNA. Each siRNA duplex was introduced into the cell lines by using lipofectamine RNAiMax (Invitrogen). Ambion ID numbers of siRNA duplex of VTI1A and STX8 were S225671 and S18183, respectively. The replicon cell line, as will be described below, was transfected with each siRNA at a final concentration of 20 nM as per the manufacturer's protocol and then seeded at 2.5×10^4 cells per well of a 24-well plate. The transfected cells were harvested at 72 h post-transfection. The Huh7OK1 cell line, as will be described below, was transfected with each siRNA at a final concentration of 20 nM as per the manufacturer's protocol and then seeded at 2.5×10^4 cells per well of a 24-well plate. The transfected cells were infected with JFH1 at an MOI of 0.05 at 24 h post-transfection. The resulting cells were harvested at the indicated time.

Quantitative Reverse-Transcription PCR (qRT-PCR)

Total RNA was prepared from the cell and culture supernatant using the RNeasy mini kit (QIAGEN, Hilden, Germany) and QIAamp Viral RNA Mini Kit (QIAGEN), respectively. First-strand cDNA was synthesized using a high capacity cDNA reverse transcription kit (Applied Biosystems, Carlsbad, CA, USA) with random primers. Each cDNA was estimated by Platinum SYBR Green qPCR Super Mix UDG (Invitrogen) as per the manufacturer's protocol. Fluorescent signals of SYBR Green were analyzed with ABI PRISM 7000 (Applied Biosystems). The HCV internal ribosomal entry site (IRES) region and human glyceraldehyde-3-phosphate dehydrogenase (GAPDH) gene were amplified with the primer pairs 5′-GAGTGTCGTGCAGCCTCCA-3′ and 5′-CACTCGCAAGCACCCTATCA-3′, and 5′-GAAGGTCGGAGTCAACGGATT-3′ and 5′-TGATGACAAGCTTCCCGTTCTC-3′, respectively.[30] The quantities of the HCV genome and the other host mRNAs were normalized with that of GAPDH mRNA. VTI1A and STX8 genes were amplified using the primer pairs 5′-TGACAGGGATGTTGCGAAGA-3′ and 5′-CAACCCACATGCAAACAGGA-3′, and 5′-TTGAAGGGGACCGAAGACAGAACCTC-3′, and 5′-TCAAAACCCAAGCCTCTGGTCTCCT-3′, respectively.

Cell Lines and Virus Infection

Cells from the Huh7OK1 cell line are highly permissive to HCV JFH1 strain (genotype 2a) infection compared to Huh 7.5.1 and exhibit the highest propagation efficiency for JFH1.[30] These cells were maintained at 37 °C in a humidified atmosphere and 5% CO_2, in Dulbecco's modified Eagle's medium (DMEM) (Sigma, St. Louis, MO, USA) supplemented with nonessential amino acids (NEAA), sodium pyruvate, and

10% fetal calf serum (FCS). The human hepatoma cell line Huh7, harboring the full genome of the HCV Con1 strain (genotype 1b), was prepared as described by Pietschmann et al.[31] We also established an Huh7 cell line harboring the subgenome of the JFH1 strain by the transfection of the plasmid pSGR-JFH1.[32] The Huh7-derived cell lines harboring a full length HCV replicon were maintained in DMEM containing 10% FCS, nonessential amino acids, sodium pyruvate, and 1 mg/mL G418 (Nakarai Tesque, Tokyo, Japan). The viral RNA of JFH1 was introduced into Huh7OK1 as described by Wakita et al.[33] The viral RNA of JFH1 derived from the plasmid pJFH1 was prepared as described by Wakita et al.[33]

Statistical Analysis

Experiments for RNAi transfection and qRT-PCR were performed three times. The estimated values were represented as the mean ± standard deviation (n = 3). The significance of differences in the means was determined by the Student's t test.

RESULTS AND DISCUSSION

Core Expression and PA28γ Knockout Induce Substantial Changes in the Expression Levels of Host Proteins Associated with HCV Infection in the Liver

The PowerBlot immunoblots showed proteins with increased or decreased levels (defined as those that displayed >1.8-fold change in abundance) in the transgenic samples relative to the WT samples and also relative to each other. In all, we identified 37 proteins with increased levels and 15 proteins with decreased levels in CoreTGvsWT, 24 proteins with increased levels and 15 proteins with decreased levels in PA28$\gamma^{-/-}$-CoreTGvsWT, and 26 proteins with increased levels and 36 proteins with decreased levels in PA28$\gamma^{-/-}$CoreTGvsCoreTG. While most proteins with altered abundance display changes between 1.8-fold and 6-fold, some proteins displayed much higher fold changes. For instance, WRN protein levels increased 17-fold in CoreTGvsWT (Table 1).

Our analysis detected changes in the abundance of proteins, known to be associated with HCV pathogenesis, in the liver samples from CoreTG compared with WT. These include Arginase I (ARG1; +2.08-fold), a liver enzyme associated with the polyamine metabolism, which is known to be overexpressed in HCV-mediated hepatocarcinogenesis;[34] STAT3 (+2.30-fold), which is directly activated by the Core and HCV-mediated oxidative stress facilitating tumorigenesis and is also essential for HCV replication;[35−37] STAT1 (+2-fold), which interacts with Core and facilitates the HCV-mediated attenuation of the host interferon signaling;[38] and MAPK14 (p38 MAPK; −2.81-fold), which is cooperatively activated by Core and ethanol in HCV infection[39] (Table 1). These results are in line with the previous observations that Core expression can induce HCV pathogenesis and hepatocarcinogenesis in transgenic mice.[2] Among other examples, BIN1, which interacts with the HCV NS5A protein and contributes to the pathogenesis of HCC,[40] was suppressed 1.88-fold in PA28$\gamma^{-/-}$CoreTGvsCoreTG; this is consistent with the lack of HCC pathogenesis in PA28$\gamma^{-/-}$CoreTG mice. Similar studies have aimed to characterize the global changes in the host transcriptome and proteome in response to HCV infection.[41−44] These studies, however, have not provided specific insights into PA28γ's roles in HCV pathogenesis. Our observations suggest that the PowerBlot assay was able to capture successfully some of the molecular signatures associated with the Core-PA28γ interplay in HCV pathogenesis.

Topological Analysis of the Extended Protein Interaction Networks

To further understand the biological significance of the differential protein levels, we retrieved PPIs for the proteins with increased and decreased levels in CoreTGvsWT, PA28$\gamma^{-/-}$CoreTGvsWT, and PA28$\gamma^{-/-}$CoreTGvsCoreTG and inferred the corresponding extended protein interaction networks for each data set using TargetMine (see Materials and Methods). First, we computed the *node degree distribution* and *characteristic/average path length* measures to capture the topology of the extended PPI networks as described earlier.[22] The degree of a protein, which corresponds to the number of its interacting partners, may often reflect its biological relevance since a better connected protein may have a higher ability of influencing biological networks via PPIs. Average path lengths provide an approximate measure of the relative ease and speed of transfer of information between the proteins in a network. The CoreTGvsWT extended network was made up of 1373 entities (proteins) with 12535 interactions, the PA28$\gamma^{-/-}$CoreTGvsWT extended network of 1057 entities with 8988 interactions, and the PA28$\gamma^{-/-}$CoreTGvsCoreTG of 1476 entities with 12871 interactions between them, respectively (Tables S3, S4). For comparison, we also derived an extended PPI network for all the non-genetic PPIs in the human genome as compiled in BioGRID and iRefindex repositories (data not shown). The average degree (defined as the number of interactions for a given protein) of the CoreTGvsWT (17.31), PA28$\gamma^{-/-}$CoreTGvsWT (16.1), and PA28$\gamma^{-/-}$CoreTGvsCoreTG (16.57) extended networks was higher than the degree inferred for the human interactome (10.17). This observation suggests that HCV infection targets several highly connected cellular proteins with an ability to influence a large number of host factors in HCV pathogenesis. The average (shortest) path lengths of the three extended networks (2.93, 2.9, and 2.97, respectively) were significantly shorter than that inferred for the human interactome (3.88), suggesting that the Core and PA28γ influenced cellular networks are more compact and inclined toward faster communication between the constituents relative to the human interactome (Figure 1). Our observations are consistent with previous studies on the protein interaction networks associated with HCV infection.[22,45]

The compactness of the HCV-influenced protein networks coupled with the ability to influence a wide array of factors in the host cellular networks may facilitate a rapid propagation of the signaling information and allow the virus to respond rapidly to the host mobilization against HCV infection.

Functional Analysis of the Extended Protein Interaction Networks

Next, we investigated the extended networks for the enrichment of specific biological associations (KEGG pathways, GO terms, and OMIM phenotypes, Tables S5, S6, and S7). The analysis of the CoreTGvsWT, PA28$\gamma^{-/-}$CoreTGvsWT, and PA28$\gamma^{-/-}$CoreTGvsCoreTG extended networks revealed an enrichment ($p \leq 0.05$) of 116, 104, and 118 KEGG pathways, respectively (Table S5). Below we describe our observations on the selected enriched biological themes of interest, chiefly associated with the PA28$\gamma^{-/-}$CoreTGvsCoreTG network. Functional associations for the host factors previously known to be associated with HCV pathogenesis and HCC are

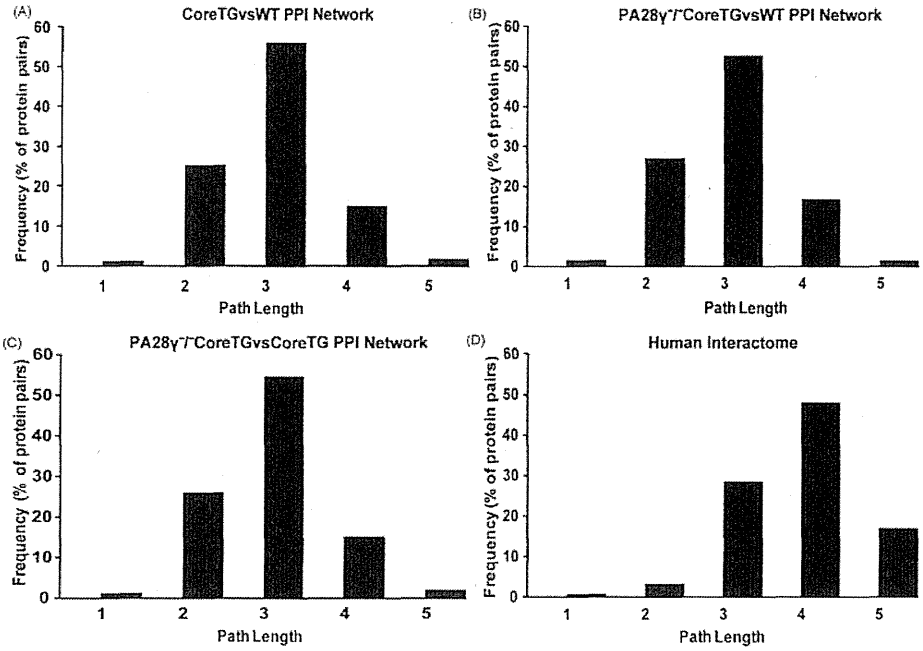

Figure 1. Graphical representation of the shortest path length distribution for (A) CoreTGvsWT extended network, (B) PA28$\gamma^{-/-}$CoreTGvsWT extended network, (C) PA28$\gamma^{-/-}$CoreTGvsCoreTG extended network, and (D) human protein interactome. The path length is represented on the x-axis, while the y-axis describes the frequency, i.e., the percentage of node (protein) pairs within the PPI network with a given shortest path length. For simplicity, only the node frequencies for path lengths 1−5 are displayed.

summarized in Table 2. Specific functional associations for the CoreTGvsWT and PA28$\gamma^{-/-}$CoreTGvsWT networks, except when discussed below, are detailed in the Supporting Information. It will highlight the biological significance of the differentially expressed proteins, their interactions, and their probable roles in HCV infection and help identify potentially novel regulators of and biomarkers for HCV pathogenesis.

Vesicular Transport

HCV infection involves the formation of the HCV replication complex in the detergent-resistant membrane (DRM) fraction or lipid rafts. These subcellular membrane fractions are utilized by some pathogens including viruses to facilitate viral entry and assembly.[46−49] HCV infection induces modifications in the host lipid raft proteome, which directly impacts HCV replication in the infected cells.[50] Core targeting to the early and late endosomes and the viral particle production requires the components of the endosome-based secretory pathways.[51,52]

CoreTGvsWT Extended Network. The PowerBlot analysis revealed the two endosomal proteins VTI1A and STX8 (KEGG Pathway "SNARE interactions in vesicular transport"; $p = 0.023$; Table S5) that were upregulated 3.25- and 1.88-fold, respectively, in CoreTGvsWT (Table 1). SNAREs are membrane-anchored proteins involved in membrane trafficking.[53] Some SNAREs may function in HCV egress by possibly facilitating the fusion of the late endosomes that carry HCV particles with the plasma membrane resulting in their release into the extracellular environment.[52] VTI1A is a SNARE involved in the vesicular transport from the late endosomes to the trans-Golgi network and forms a SNARE complex with STX16 and VAMP4 (Table S4).[54,55] STX8 is involved in the protein trafficking from the early to the late endosomes and exocytosis and forms a SNARE complex with STX7, VAMP8, and VTI1B.[55,56] A reduction in the expression of STX7, which interacts with both VTI1A and STX8 (Figure 2; Table S4), decreases HCV replication.[50] Taken together, the increased abundances of VTI1A and STX8 in CoreTGvsWT, but not PA28$\gamma^{-/-}$CoreTGvsWT, suggest potentially crucial roles of the two proteins in the HCV life cycle.

PA28$\gamma^{-/-}$CoreTGvsCoreTG Extended Network. Syntaxin 11 (STX11), a SNARE, was upregulated 3.52-fold in PA28$\gamma^{-/-}$CoreTGvsCoreTG (Table 1) and was mapped to the enriched KEGG Pathway "SNARE interactions in vesicular transport" ($p = 0.003$; Table S5). STX11 associates with the late endosomes and functions in the essential trafficking pathways (such as cytokine secretion) in the immune cells, with enhanced STX11 expression contributing to increased NK-cell mediated cytotoxicity.[57−61] STX11 binds with the SNARE VTI1B (Figure 3, Table S4) and regulates its participation the Q-SNARE complexes and, thus, the endocytic and exocytic trafficking in the macrophages. Overexpression of STX11 alters the VTI1B binding to STX6 and STX8 and likely reduces the endosomal transport to the cell surface.[57]

USO1, a Golgi-associated peripheral membrane protein, was decreased 2.05-fold in PA28$\gamma^{-/-}$CoreTGvsCoreTG (Table 1) and was identified as a significant linking component of the PA28$\gamma^{-/-}$CoreTGvsCoreTG SNARE network (Figure 3). USO1 plays an important role in ER to Golgi trafficking and its knockdown leads to the disintegration of the Golgi complex.[62,63] Decreased USO1 levels in PA28$\gamma^{-/-}$CoreTGvsCoreTG may, therefore, significantly impact the endosomal pathways associated with HCV release.

PA28γ knockdown impairs the production of the infectious HCV particles (but not replication) in the JFH1 (HCV genotype 2a) infected cells, largely due to the deregulation of the E6AP-dependent Core degradation, which contributes to an antiviral response.[14] Our analysis suggests a potentially novel